tion involves a large displacement of H1, stabilized by new salt bridges with β-tubulin, and an opening of CC1 at the base of the stalk (Fig. 4E). The movements of H1 and CC1 likely constrain the registries that can be explored by the stalk, biasing the distribution toward the high-affinity α registry (Fig. 4E). Propagation of this signal to the head would elicit conformational changes that produce a movement of the linker domain and a displacement of dynein toward the MT minus end.

Our analysis of dynamic salt bridges reveals that cytoplasmic dynein has been selected for submaximal processivity. Whereas kinesin has diversified its functional repertoire through gene duplication and divergence (*33*), cytoplasmic dynein is expressed from a single locus and may have evolved suboptimal processivity to increase the dynamic range of its regulation. High processivity could also be detrimental when multiple dyneins and kinesins must balance their actions on a single cargo (*34*). Consistent with this idea, intraflagellar dyneins, responsible for long, unidirectional transport within cilia (*35*, *36*), contain neutral or basic residues at the equivalent of H6-E3378 (fig. S12), which would likely increase their processivity.

References and Notes

1. I. R. Gibbons, *Cell Motil. Cytoskeleton* **32**, 136 (1995).
2. P. Höök, R. B. Vallee, *J. Cell Sci.* **119**, 4369 (2006).
3. R. D. Vale, *Cell* **112**, 467 (2003).
4. R. B. Vallee, G. E. Seale, J.-W. Tsai, *Trends Cell Biol.* **19**, 347 (2009).
5. R. B. Vallee, J. C. Williams, D. Varma, L. E. Barnhart, *J. Neurobiol.* **58**, 189 (2004).
6. S. A. Burgess, M. L. Walker, H. Sakakibara, P. J. Knight, K. Oiwa, *Nature* **421**, 715 (2003).
7. A. J. Roberts *et al.*, *Cell* **136**, 485 (2009).
8. I. R. Gibbons, B. H. Gibbons, G. Mocz, D. J. Asai, *Nature* **352**, 640 (1991).
9. T. Kon, M. Nishiura, R. Ohkura, Y. Y. Toyoshima, K. Sutoh, *Biochemistry* **43**, 11266 (2004).
10. S. L. Reck-Peterson, R. D. Vale, *Proc. Natl. Acad. Sci. U.S.A.* **101**, 1491 (2004).
11. S. L. Reck-Peterson *et al.*, *Cell* **126**, 335 (2006).
12. T. Shima, T. Kon, K. Imamula, R. Ohkura, K. Sutoh, *Proc. Natl. Acad. Sci. U.S.A.* **103**, 17736 (2006).
13. A. P. Carter, C. Cho, L. Jin, R. D. Vale, *Science* **331**, 1159 (2011).
14. T. Kon, K. Sutoh, G. Kurisu, *Nat. Struct. Mol. Biol.* **18**, 638 (2011).
15. M. P. Koonce, *J. Biol. Chem.* **272**, 19714 (1997).
16. M. A. Gee, J. E. Heuser, R. B. Vallee, *Nature* **390**, 636 (1997).
17. A. P. Carter *et al.*, *Science* **322**, 1691 (2008).
18. I. R. Gibbons *et al.*, *J. Biol. Chem.* **280**, 23960 (2005).
19. T. Kon *et al.*, *Nat. Struct. Mol. Biol.* **16**, 325 (2009).
20. T. Kon *et al.*, *Nature* **484**, 345 (2012).
21. N. Mizuno *et al.*, *EMBO J.* **23**, 2459 (2004).
22. C. V. Sindelar, K. H. Downing, *J. Cell Biol.* **177**, 377 (2007).
23. C. V. Sindelar, K. H. Downing, *Proc. Natl. Acad. Sci. U.S.A.* **107**, 4111 (2010).
24. D. B. Wells, A. Aksimentiev, *Biophys. J.* **99**, 629 (2010).
25. J. Löwe, H. Li, K. H. Downing, E. Nogales, *J. Mol. Biol.* **313**, 1045 (2001).
26. L. G. Trabuco, E. Villa, K. Mitra, J. Frank, K. Schulten, *Structure* **16**, 673 (2008).
27. L. G. Trabuco, E. Villa, E. Schreiner, C. B. Harrison, K. Schulten, *Methods* **49**, 174 (2009).
28. J. Schlitter, M. Engels, P. Krüger, *J. Mol. Graph.* **12**, 84 (1994).
29. S. Uchimura, Y. Oguchi, Y. Hachikubo, S. Ishiwata, E. Muto, *EMBO J.* **29**, 1167 (2010).
30. M. P. Koonce, I. Tikhonenko, *Mol. Biol. Cell* **11**, 523 (2000).
31. Z. Wang, M. P. Sheetz, *Biophys. J.* **78**, 1955 (2000).
32. L. McNaughton, I. Tikhonenko, N. K. Banavali, D. M. LeMaster, M. P. Koonce, *J. Biol. Chem.* **285**, 15994 (2010).
33. E. M. Dagenbach, S. A. Endow, *J. Cell Sci.* **117**, 3 (2004).
34. M. A. Welte, *Curr. Biol.* **14**, R525 (2004).
35. C. Iomini, V. Babaev-Khaimov, M. Sassaroli, G. Piperno, *J. Cell Biol.* **153**, 13 (2001).
36. J. A. Laib, J. A. Marin, R. A. Bloodgood, W. H. Guilford, *Proc. Natl. Acad. Sci. U.S.A.* **106**, 3190 (2009).

Acknowledgments: We thank A. Carter (Laboratory of Molecular Biology-Medical Research Council) for reagents and advice, C. Sindelar (Yale), V. Ramey [University of California (UC)–Berkeley], E. Egelman (University of Virginia), and R. Sinkovits (UC–San Diego) for sharing processing scripts and helpful advice; M. Sotomayor (Harvard) and R. Gaudet (Harvard) for advice concerning MD; J. Hogle (Harvard), M. Strauss (Harvard), and M. Wolf (Harvard) for help with film and the use of a film scanner; and E. Nogales (UC-Berkeley), N. Francis (Harvard), and D. Pellman (Harvard) for critically reading the manuscript, as well as all the members of the Leschziner and Reck-Peterson Labs for advice and helpful discussions. EM data were collected at the Center for Nanoscale Systems (CNS), a member of the National Nanotechnology Infrastructure Network (NNIN), which is supported by the National Science Foundation under NSF award no. ECS-0335765. CNS is part of Harvard University. MD simulations were run on the Odyssey cluster supported by the Faculty of Arts and Sciences Science Division Research Computing Group, Harvard University. S.L.R.-P. is funded by the Rita Allen Foundation, the Harvard Armenise Foundation, and an NIH New Innovator award (1 DP2 OD004268-1). A.E.L. was funded in part by a Research Fellowship from the Alfred P. Sloan Foundation. R.H.-L. was supported in part by Consejo Nacional de Ciencia y Tecnología and Fundación México en Harvard. The cryo-EM map was deposited at the EM Data Bank (EMDB-5439) and pseudo-atomic models at the Protein Data Bank (PDB-3J1T and -3J1U).

Supplementary Materials

www.sciencemag.org/cgi/content/full/337/6101/1532/DC1
Materials and Methods
Figs. S1 to S12
Tables S1 to S3
References (*37*–*53*)
Movies S1 to S6

2 May 2012; accepted 20 July 2012
10.1126/science.1224151

Specifying and Sustaining Pigmentation Patterns in Domestic and Wild Cats

Christopher B. Kaelin,[1,2]* Xiao Xu,[3,4]* Lewis Z. Hong,[2] Victor A. David,[3] Kelly A. McGowan,[2] Anne Schmidt-Küntzel,[3,5] Melody E. Roelke,[3,6] Javier Pino,[7] Joan Pontius,[3,6] Gregory M. Cooper,[1] Hermogenes Manuel,[2] William F. Swanson,[8] Laurie Marker,[5] Cindy K. Harper,[9] Ann van Dyk,[10] Bisong Yue,[4] James C. Mullikin,[11] Wesley C. Warren,[12] Eduardo Eizirik,[13,14] Lidia Kos,[7] Stephen J. O'Brien,[3]†‡ Gregory S. Barsh,[1,2]† Marilyn Menotti-Raymond[3]

Color markings among felid species display both a remarkable diversity and a common underlying periodicity. A similar range of patterns in domestic cats suggests a conserved mechanism whose appearance can be altered by selection. We identified the gene responsible for tabby pattern variation in domestic cats as *Transmembrane aminopeptidase Q* (*Taqpep*), which encodes a membrane-bound metalloprotease. Analyzing 31 other felid species, we identified *Taqpep* as the cause of the rare king cheetah phenotype, in which spots coalesce into blotches and stripes. Histologic, genomic expression, and transgenic mouse studies indicate that paracrine expression of *Endothelin3* (*Edn3*) coordinates localized color differences. We propose a two-stage model in which *Taqpep* helps to establish a periodic pre-pattern during skin development that is later implemented by differential expression of *Edn3*.

The molecular basis and evolutionary variation of periodic mammalian color patterns have been difficult to investigate from genetic crosses of model organisms. Domestic cats (*Felis catus*) exhibit heritable variation of tabby markings—mackerel versus blotched—that provide an opportunity for such genetic analysis (*1*). Tabby markings are a composite of two features: (i) a light background component in which individual hairs have extensive light bands, and (ii) a superimposed darker component in which hairs have little or no banding. In mackerel cats, the dark component is organized into narrow vertical stripes with a constant and regular spacing, whereas in blotched cats, the dark component is expanded into a less organized structure with wide whorls (Fig. 1A). Periodic color patterns in other felids may represent the same process; for example, dark tabby markings in domestic cats may be homologous to black stripes or spots in tigers or cheetahs, respectively (*2*).

A logical explanation for tabby patterning involves the Agouti-melanocortin receptor system, in which Agouti protein, a paracrine signaling molecule released from dermal papillae, acts on overlying hair follicle melanocytes to inhibit the melanocortin 1 receptor (Mc1r), causing a switch from the production of black/brown eumelanin to red/yellow pheomelanin (*3*, *4*). According to this hypothesis, dark tabby stripes are areas in which Agouti signaling is suppressed or surmounted during hair growth and regeneration. However, known components of the Agouti-melanocortin

pathway do not affect the shape of tabby patterns (*1*, *2*, *5*, *6*). Instead, the difference between mackerel and blotched is controlled by a single locus, *Tabby* (*Ta*), whose genetic position does not suggest an obvious candidate gene (*7*) but whose effects could be manifested via differential control of melanocortin signaling.

The 3X cat genome assembly is not contiguous across the *Tabby* linkage interval (*7*), but comparison to homologous regions in the dog and human genomes suggests a candidate interval of ~5 Mb in length (fig. S1A). Old World wild cats, from which domestic cats arose ~10,000 years ago (*8*), exhibit a mackerel-like pattern. However, the blotched pattern is common in many modern breeds, suggesting that one or a few Ta^b causal variants would lie in a region of reduced allelic variation due to recent selection. We used comparative genomic information to identify single-nucleotide polymorphisms (SNPs) in the candidate interval, then genotyped and analyzed 16 blotched (Ta^b/Ta^b) and 33 mackerel (Ta^M/Ta^M or Ta^M/Ta^b) animals from a feral population in northern California. Five SNPs from a 180-kb interval on chrA1 showed significant association (P range = 9×10^{-4} to 3.2×10^{-9}) (fig. S1B).

Twenty-four markers genotyped in and around the associated region in 58 blotched and 19 mackerel cats indicated that all blotched animals shared a common haplotype extending for 244 kb, whereas mackerel samples exhibited several haplotypes within the same interval (figs. S1C and S2). Coding sequences from three genes are located within the 244-kb interval: *Commd10*, *LOC644100*, and a third gene whose human ortholog has been referred to as both *Aminopeptidase Q* and *Laeverin* (*9*). No sequence alterations were observed in *LOC644100* or *Commd10*, but most blotched cats carried a nonsense mutation, W841X (Fig. 1B, fig. S2, and table S1), in exon 17 of the third gene. We subsequently identified two additional variants in the same gene, S59X and D228N (Fig. 1B, fig. S2, and table S1). This gene is expressed in developing felid skin, and its loss of function causes a loss of color pattern periodicity

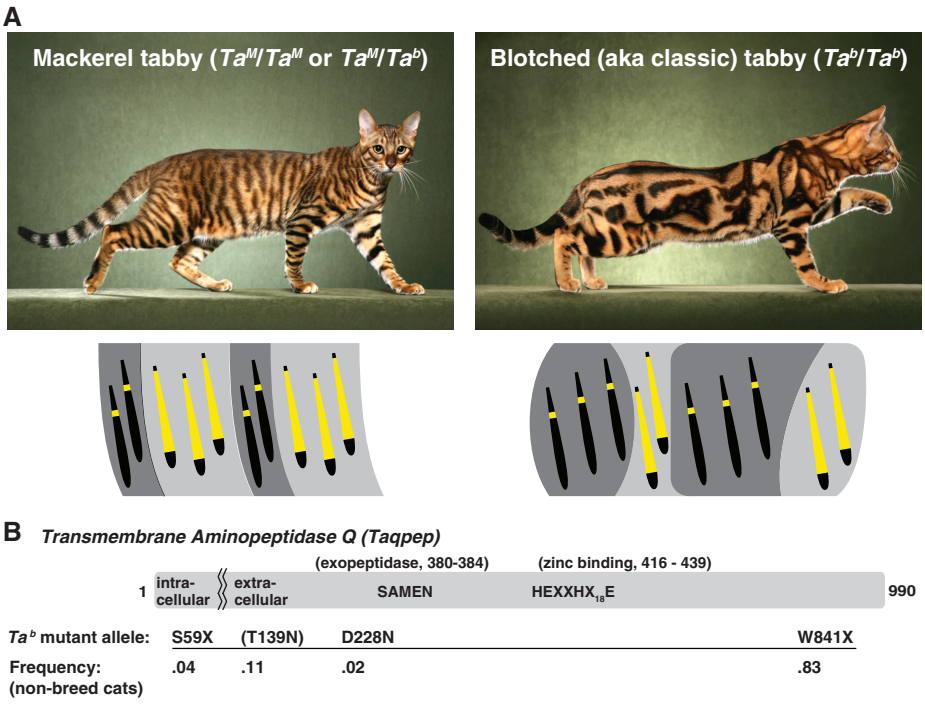

Fig. 1. (A) Allelic variation at *Tabby* [mackerel (Ta^M) is dominant to blotched (Ta^b)] controls the arrangement of dark- and light-colored areas. Diagrams indicate how the distribution of black or brown eumelanin versus yellow or pale pheomelanin within individual hairs underlies the macroscopic color patterns, although in reality cat hairs frequently exhibit multiple pheomelanic bands. (**B**) *Taqpep* encodes a type II membrane protein with aminopeptidase activity encoded by the ectodomain. Mutant allele frequencies are from a survey of 119 feral and outbred cats (table S1). The T139N allele is associated (P = 0.0017, Fisher's exact test) with an atypical swirled pattern but is incompletely penetrant (table S1 and fig. S2).

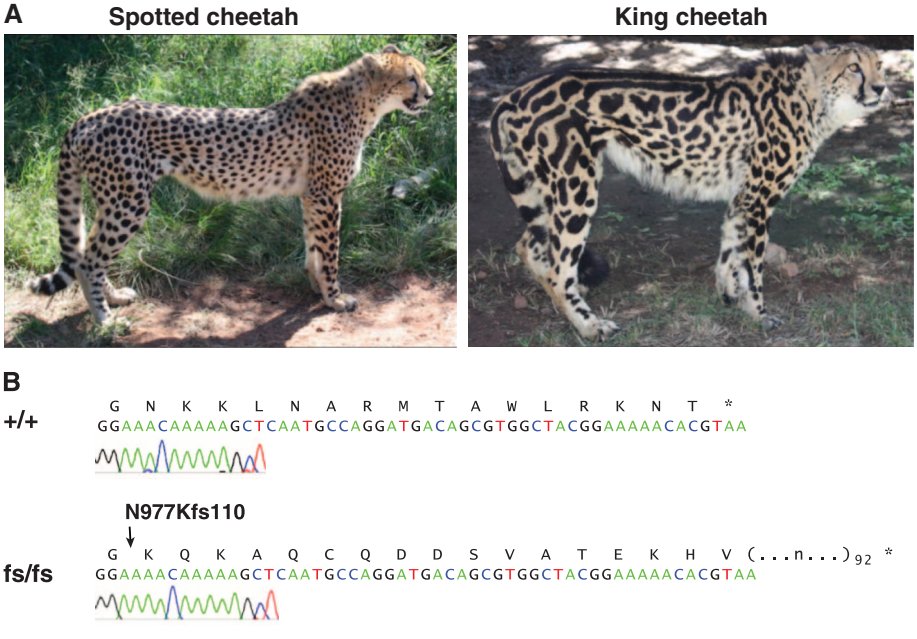

Fig. 2. (**A**) Black-haired areas are larger, more irregular, and associated with dorsal stripes in the king cheetah. (**B**) Chromatogram of *Taqpep* cDNA from a spotted (+/+) as compared to a king (fs/fs) cheetah.

[1]HudsonAlpha Institute for Biotechnology, Huntsville, AL 35806, USA. [2]Department of Genetics, Stanford University, Stanford, CA, 94305, USA. [3]Laboratory of Genomic Diversity, Frederick National Laboratory for Cancer Research, Frederick, MD 21702, USA. [4]Sichuan Key Laboratory of Conservation Biology on Endangered Wildlife, College of Life Sciences, Sichuan University, Sichuan 610064, China. [5]Cheetah Conservation Fund, Post Office Box 1755, Otjiwarongo, Namibia. [6]SAIC-Frederick, Frederick National Laboratory for Cancer Research, Frederick, MD 21702, USA. [7]Department of Biological Sciences, Florida International University, Miami, FL 33199, USA. [8]Center for Conservation and Research of Endangered Wildlife, Cincinnati Zoo & Botanical Garden, Cincinnati, OH 45220, USA. [9]Veterinary Genetics Laboratory, Faculty of Veterinary Science Onderstepoort, University of Pretoria, Pretoria, South Africa. [10]The Ann van Dyk Cheetah Centre, De Wildt, South Africa. [11]Comparative Genomics Unit, National Human Genome Research Institute, National Institutes of Health, Rockville, MD 20892, USA. [12]The Genome Center, Washington University in St. Louis, St. Louis, MO 63108, USA. [13]Faculdade de Biociências, Pontifícia Universidade Católica do Rio Grande do Sul, Porto Alegre, Rio Grande do Sul 90619-900, Brazil. [14]Instituto Pró-Carnívoros, Atibaia, Brazil.

*These authors contributed equally to this work.
†To whom correspondence and requests for materials should be addressed. E-mail: gbarsh@hudsonalpha.org (G.S.B.); lgdchief@gmail.com (S.J.O'B.).
‡Present address: Theodosius Dobzhansky Center for Genome Informatics, St. Petersburg State University, St. Petersburg, Russia.

without obvious effects on other organ systems. We refer to this gene as *Transmembrane Aminopeptidase Q* (*Taqpep*) and the protein product as Tabulin to reflect its organismal function.

Taqpep encodes a type II membrane-spanning protein of the M1 aminopeptidase family, whose members are characterized by the presence of GAMEN exopeptidase (SAMEN in Taqpep) and $HEXXHX_{18}E$ zinc-binding motifs in their extracellular domains (Fig. 1B) (*9*). In feral cats, we observed homozygosity or compound heterozygosity for the Ta^b S59X or W841X alleles in 58 out of 58 (58/58) blotched animals, with no phenotypic distinction among the different genotypic classes, compared to 51/51 mackerel cats that carried 0 or 1 Ta^b alleles (table S1). A third Ta^b allele, D228N, was found to cosegregate with the blotched phenotype in a research colony (fig. S2D). In feral cats, we also observed two variants at codon 139, one of which, T139N, was significantly associated (P = 0.0017, Fisher's exact test) with an atypical swirled pattern (figs. S2 and S4D and table S1) and therefore may represent hypomorphic or neomorphic activity. Overall, the mutant W841X allele predominates and is responsible for the strong haplotype signature (fig. S1C), although the S59X allele occurs on the same haplotype background, in trans to W841X (fig. S2).

Cheetahs (*Acinonyx jubatus*) with the rare king pattern were originally described as a distinct felid species (*10*) but were later recognized as having a monogenic trait with an autosomal recessive mode of inheritance (*11*). In king cheetahs, the black spots coalesce into larger areas, and multiple longitudinal black stripes appear on the dorsum (Fig. 2A). Wild king cheetahs have been sighted only in a small area of sub-Saharan Africa (fig. S3) (*11*). *Taqpep* genomic sequence from a captive king cheetah in North America revealed a base pair insertion in exon 20, predicting a frameshift that replaces what would normally be the carboxy-terminal 16 amino acids with 109 new residues (N977Kfs110, Fig. 2B). Additional DNA samples from captive cheetahs in a large pedigree demonstrated complete cosegregation of the king pattern with the N977Kfs110 mutation [LOD (logarithm of odds) score = 5.7], and further revealed that the mutant allele was introduced into the pedigree by one homozygous and two heterozygous animals (fig. S3). We did not detect the N977Kfs110 mutation in wild cheetahs caught in Namibia (n = 191), Tanzania (n = 23), or Kenya (n = 3).

Depictions of tabby markings from the Middle Ages are mostly mackerel, but the blotched phenotype increased to a sufficiently high frequency to be described by Linnaeus in 1758 as characteristic for the domestic cat, predating the formation of most modern breeds. We examined the predicted Tabulin sequence in 351 cats from 24 breeds (table S2) and observed that the W841X allele is polymorphic in most breeds of Western origin, but rare or absent in Eastern breeds. The high allele frequency for W841X in Abyssinian (1.0), Birman (0.71), and Himalayan (0.77) cats is especially notable, because tabby markings in these breeds are masked by epistatic interactions. The S59X allele, probably representing a complete ablation of protein function, is most common in Norwegian Forest Cats, and we observed one S59X/S59X homozygote with a blotched phenotype.

We determined *Taqpep* sequence for 31 wild felid species, identifying 130 synonymous and 64 nonsynonymous predicted substitutions (fig. S4A). We assessed the potential functional impact of the nonsynonymous substitutions with multivariate analysis of protein polymorphism (MAPP) (*12*), a quantitative approach that takes into account both evolutionary conservation and side-chain physicochemical properties. A MAPP score >10 indicates a likely impact on protein function, and the T139N and D228N substitutions associated with atypical swirled and blotched mutant phenotypes, respectively, in the domestic cat yield MAPP scores of 11 ($P = 1.5 \times 10^{-3}$) and 14 ($P = 3.9 \times 10^{-4}$) (fig. S4B). In contrast, the T139A variant in the domestic cat (which does not affect pattern) yields a MAPP score of 3.8. The black-footed cat (*Felis nigripes*) is a clear outlier from other Felidae, with five lineage-specific nonsynonymous substitutions and a combined MAPP score of 50 (fig. S4C). *F. nigripes* exhibits a spotting phenotype that is similar to the atypical swirled pattern associated with the T139N allele in domestic cats (fig. S4D); thus, recent evolution of *Taqpep* in *F. nigripes* may contribute to its characteristic pattern.

To investigate how color patterns are implemented, we examined fetal cat skin at 3, 5, and 7 weeks of gestation, and observed that the first histologic indication of tabby markings coincides with their external appearance at 7 weeks, when follicle architecture is established and hair shafts begin to protrude through the epidermal surface

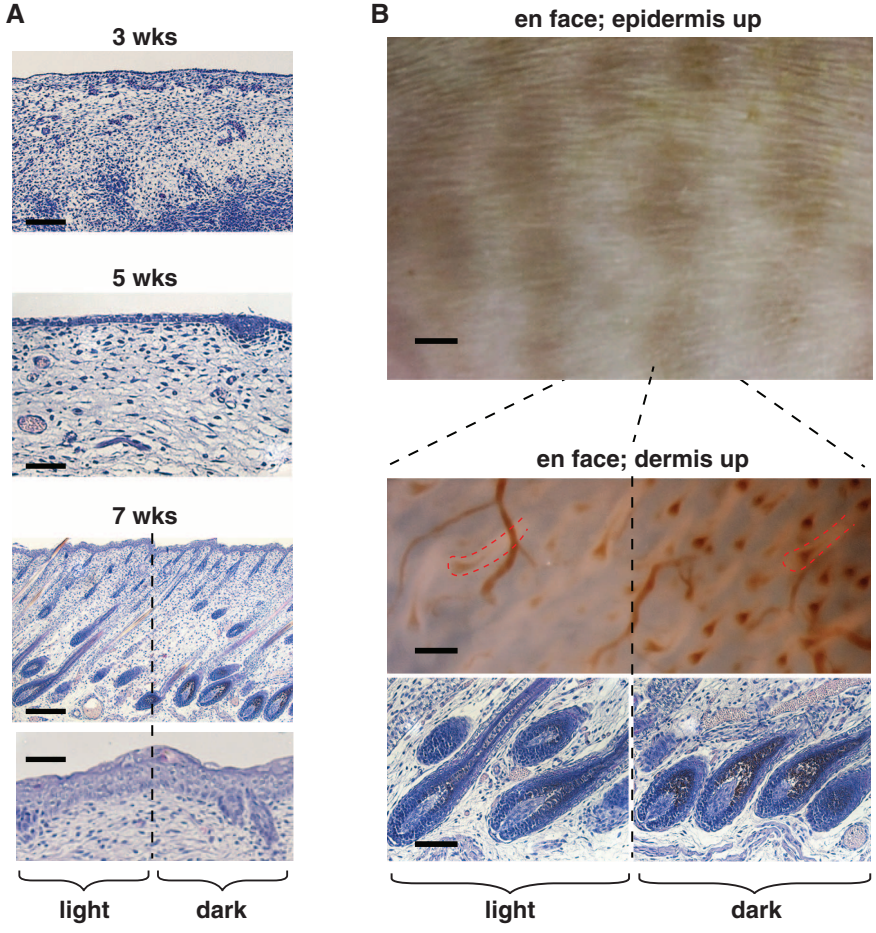

Fig. 3. Skin sections of fetal cats [(**A**), at 3, 5, and 7 weeks of gestation] stained with hematoxylin and eosin, together with unstained flat-mount (en face) skin preparations of fetal cats [(**B**), at 7 weeks of gestation]. The 7-week images in (B) are from an orange (*O/Y* or *O/O*) individual, which allows the dark component of the tabby pattern (which is orange-colored) to be more easily visualized. In the trans-illuminated "dermis-up" panel, hair follicle outlines (dashed red lines) appear light-colored; melanin incorporation and blood vessels appear dark-colored. Scale bars in (A), 150, 50, and 250 μm in 3-, 5-, and 7-week fetal cat sections, respectively, and 50 μm in the 7-week epidermis close-up. Scale bars in (B), 2 mm, 100 μm, and 600 μm in epidermis-up, follicle histology, and dermis-up panels, respectively.

(Fig. 3). At this stage, the boundary between dark and light tabby components reflects differences in the amount of melanin deposition, with no apparent difference in cell type; melanocytes are present in both dark and light areas but produce more melanin in dark areas. Furthermore, the density and architecture of hair follicles are independent of localization to dark and light areas (Fig. 3B). This suggests that tabby markings arise from spatial variation in transcriptional activity rather than cell type distribution.

We used the EDGE (EcoP15I-tagged Digital Gene Expression) (*13*) method for gene expression profiling to examine the transcriptome of cheetah skin, in which there are sharp boundaries between black spots and the yellow interspot areas and for which multiple skin biopsies were available for study. Cheetah skin exhibits an unusual histologic architecture; the epidermis is heavily pigmented, and hair follicles are organized in clusters with extensive accessory structures (Fig. 4A and fig. S5A). However, the number and size of follicle clusters, as well as the number of epidermal pigment cells, do not vary between black-haired and yellow-haired areas (fig. S5B). Based on a previous analysis of EDGE results from a single cheetah, we hypothesized that black coloration involves localized alterations of genes downstream of Mc1r signaling (*13*). Biopsies of yellow- and black-colored areas from five different animals enabled a genome-wide approach, in which the expression of 14,014 genes could be measured across a 10^6-fold dynamic range (Fig. 4B). At a false discovery rate (q) < 0.05, we identified 74 differentially expressed genes (tables S7 and S8).

Among 60 genes up-regulated in black as compared to yellow cheetah skin, 7 are melanocyte-specific, of which 4 [*Tyr* (4.9-fold, $q = 3.8 \times 10^{-19}$), *Silv* (7.3-fold, $q = 1 \times 10^{-36}$), *Dct* (3.2-fold, $q = 5.3 \times 10^{-8}$), and *Tyrp1* (3.1-fold, $q = 1.7 \times 10^{-5}$)] encode pigment type-switching components (*14*, *15*). Genes that encode ligands or regulators of Mc1r signaling are not differentially expressed between yellow and black cheetah skin (Fig. 4B and table S7). However, one of the nonmelanocytic genes up-regulated in black as compared to yellow cheetah skin (4.9-fold, $q = 2.1 \times 10^{-4}$), *Edn3*, a paracrine hormone expressed mostly by mesenchymal cells that promotes differentiation and proliferation of melanocytes and other neural

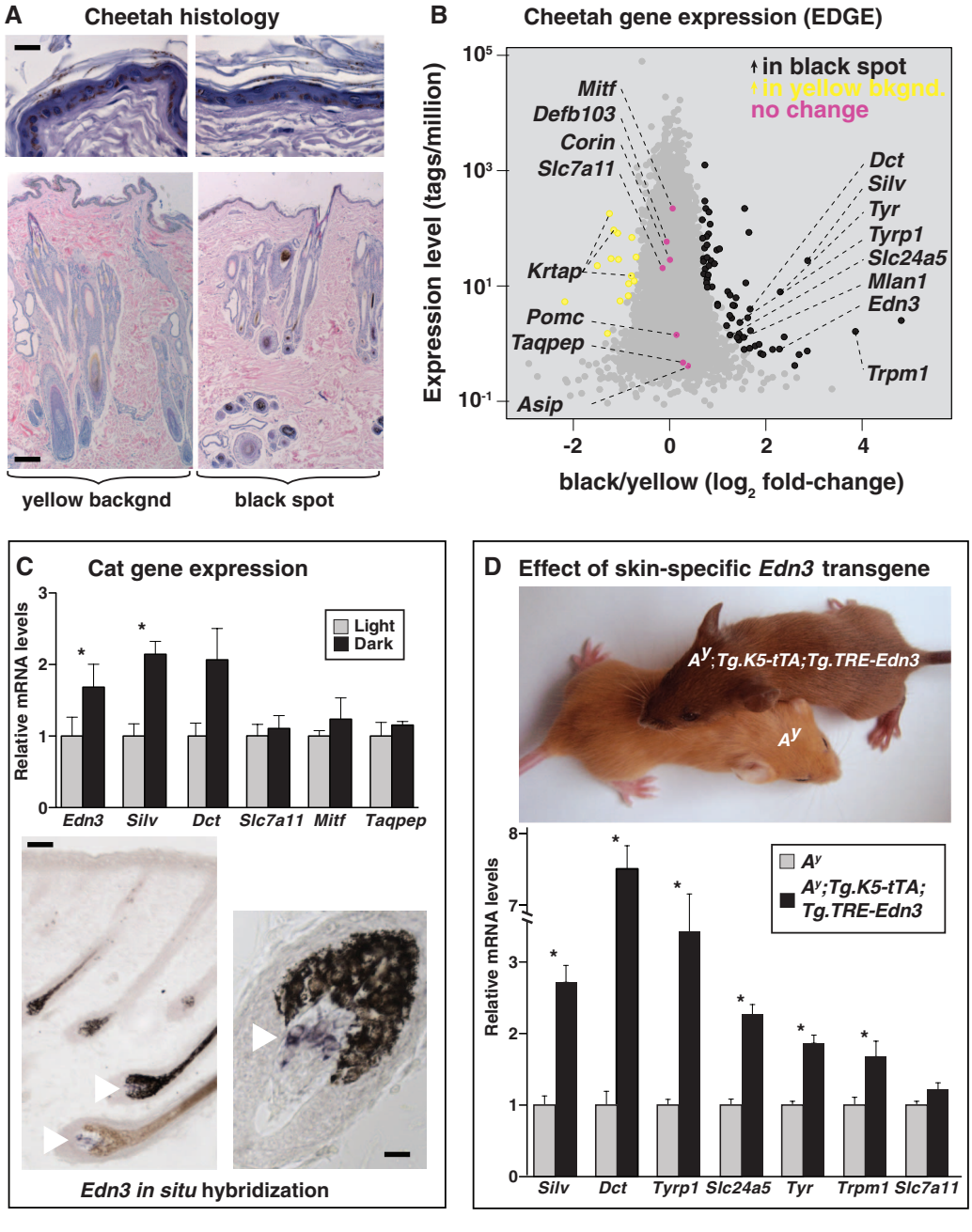

Fig. 4. (**A**) A cheetah skin biopsy that includes a black-yellow boundary (also see fig. S6). (**B**) EDGE (*13*) determination of differential gene expression in black- as compared to yellow-colored areas of cheetah skin. Transcript frequency (observations per million sequence reads, mean of five samples) is plotted as a function of differential expression. The 74 genes with significant differential expression are shown in black or yellow (FDR < 0.05, see methods and tables S8 and S9); 7 additional pigmentation genes that are not differentially expressed are shown in pink. (**C**) Relative mRNA levels (mean ± SE) for the indicated genes as assessed by qRT-PCR from paired samples ($n = 4$) of dark and light neonatal tabby skin; *$P < 0.05$ (dark versus light, two-tailed t test). Dermal papilla expression of *Edn3* mRNA (purple stain, white arrows) as detected by in situ hybridization, from a brown tabby individual. The left panel illustrates the expression of *Edn3* mRNA in both pheomelanin- and eumelanin-containing follicles. (**D**) Phenotypes of 2-week-old mice of the indicated genotypes. Relative mRNA levels (mean ± SE) for the indicated genes from qRT-PCR of cDNA from control ($n = 4$) and transgenic ($n = 4$) mice are shown; *$P < 0.05$ (A^y versus A^y;*Tg.K5-tTA;Tg.TRE-Edn3*, two-tailed t test). Scale bars in (A), 40 and 200 μm in epidermis and whole-skin sections, respectively. In (C), 60 and 20 μm in left and right panels, respectively.

crest derivatives, is a candidate for the coordination of spatial variation in hair color. A hypermorphic mutation of Gnaq, the second messenger through which Edn3 acts, causes the accumulation of dermal melanocytes during embryogenesis and converts yellow hair to black in postnatal mice (*16*, *17*).

Quantitative reverse transcription polymerase chain reaction (qRT-PCR) confirmed that the expression of *Edn3* and *Silv* was increased in black-colored as compared to yellow-colored areas of cheetah skin; we also observed similar increases in a single leopard skin sample (fig. S5C). In neonatal skin from domestic cats (in which there is a high proportion of anagen follicles), *Edn3* mRNA expression was also ~twofold higher in dark as compared to light areas (Fig. 4C), and in situ hybridization revealed that expression was restricted to the dermal papilla, a permanent portion of the hair follicle.

In A^y mutant mice, which express high levels of Agouti protein and produce pheomelanin instead of eumelanin, we confirmed that an *Edn3* transgene (*18*) converts yellow hair to dark brown–colored hair (Fig. 4D). Using qRT-PCR, we observed that the *Edn3* transgene in mice also caused increased expression of the same melanocyte-specific genes that are overexpressed in black-colored areas of cheetah skin (Fig. 4B). Thus, increased expression of *Edn3* in transgenic mice probably recapitulates both the coat color and melanocytic gene expression phenotypes observed in cheetah skin, which suggests that localized expression of *Edn3* during felid hair follicle growth serves as a master regulator of spatial hair color differences associated with tabby markings.

In the skin of neonatal domestic cats and adult cheetahs, *Taqpep* mRNA is expressed at low levels that do not differ between dark and light areas (Fig. 4, B and C). In mice, levels of whole-embryo *Taqpep* mRNA as measured by qRT-PCR increased progressively during gestation and were highest in postnatal skin (fig. S6). In situ hybridization to mouse embryos (at embryonic days 10.5 to 17.5) and to fetal cat skin at 3, 5, 6, and 7 weeks of gestation did not reveal localization of *Taqpep* mRNA to any specific cell type or region.

Because tabby markings are apparent soon after the time when melanocytes enter hair follicles (Fig. 3A), the effects of *Taqpep* on pattern morphology must occur at or before follicle development and are therefore likely to be mediated by epithelial or mesenchymal cells. Our results suggest that *Taqpep* is required to establish the periodicity of tabby markings during skin development (Fig. 5A), and that the "tabby marking" identity of a particular region is implemented and maintained by the ability of dermal papilla cells to sustain high versus low levels of *Edn3* production throughout subsequent hair cycles (Fig. 5B). This model also helps to explain why, in contrast to many periodic color patterns in fish, which are mediated by and depend on direct contact between pigment cells (*19*–*21*), tabby markings change in size but not number during organismal growth.

Our findings also provide a mechanistic explanation for epistasis relationships between *Agouti*, *Mc1r*, and *Tabby*. Homozygosity for a loss-of-function *Agouti* allele is associated with a "ghost pattern" in which Tabby stripes are difficult or impossible to visualize, because eumelanogenic genes such as *Tyr*, *Tyrp1*, *Dct*, and *Pmel* are already upregulated. The ghost pattern becomes apparent, however, in animals that are doubly mutant for *Agouti* and *Mc1r* (*5*), because endothelin and melanocortin signaling act in parallel (fig. S7). A system in which distinct paracrine signaling pathways—endothelins via a $G\alpha_q$-coupled receptor and melanocortins via a $G\alpha_s$-coupled receptor—converge on overlapping cellular machinery could explain more complicated phenotypes, in which pheomelanin-rich yellow versus eumelanin-rich black areas exhibit both periodic and regional fluctuation, such as spots or stripes of alternative pigment types overlaid on a background of dorsoventral differences, as is apparent in leopards, jaguars, and tigers. Further studies of color pattern in domestic-wild cat hybrids offer the opportunity to study these complex color markings and add to our knowledge of how felids acquire their color patterns.

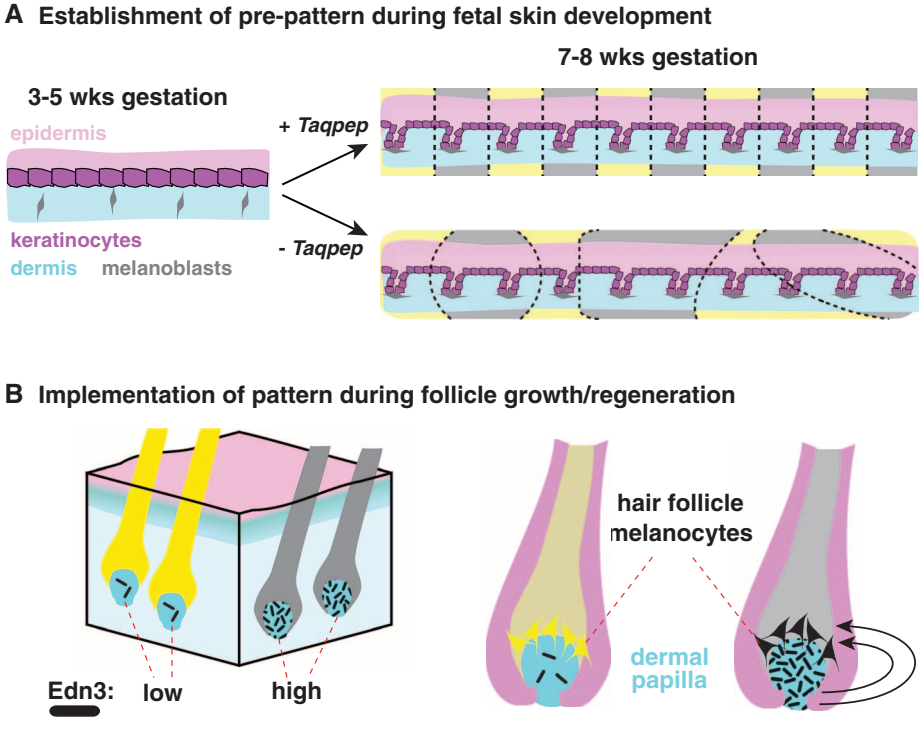

Fig. 5. A tabby pre-pattern is established at or before hair follicle development (**A**), specifying regions as dark (gray-colored) or light (yellow-colored). In the absence of *Taqpep*, dark regions are expanded, and there is less periodicity. Regional identity is manifested and implemented (**B**) by differential expression of *Edn3* in the dermal papilla, a permanent part of the hair follicle that releases paracrine factors to act on overlying melanocytes. Yellow and black pigment are synthesized by melanocytes in hair follicles that produce low and high levels of *Edn3*, respectively.

References and Notes

1. T. D. Lomax, R. Robinson, *J. Hered.* **79**, 21 (1988).
2. A. G. Searle, *Comparative Genetics of Coat Color in Mammals* (Academic Press, New York, 1968).
3. S. E. Millar, M. W. Miller, M. E. Stevens, G. S. Barsh, *Development* **121**, 3223 (1995).
4. I. J. Jackson, *Annu. Rev. Genet.* **28**, 189 (1994).
5. M. Peterschmitt, F. Grain, B. Arnaud, G. Deléage, V. Lambert, *Anim. Genet.* **40**, 547 (2009).
6. E. Eizirik *et al.*, *Curr. Biol.* **13**, 448 (2003).
7. E. Eizirik *et al.*, *Genetics* **184**, 267 (2010).
8. C. A. Driscoll *et al.*, *Science* **317**, 519 (2007).
9. M. Maruyama *et al.*, *J. Biol. Chem.* **282**, 20088 (2007).
10. R. I. Pocock, *Proc. Zool. Soc. London* **97**, 245 (1927).
11. R. J. van Aarde, A. van Dyk, *J. Zool.* **209**, 573 (1986).
12. E. A. Stone, A. Sidow, *Genome Res.* **15**, 978 (2005).
13. L. Z. Hong, J. Li, A. Schmidt-Küntzel, W. C. Warren, G. S. Barsh, *Genome Res.* **21**, 1905 (2011).
14. C. S. April, G. S. Barsh, *Pigment Cell Res.* **19**, 194 (2006).
15. T. Kobayashi *et al.*, *J. Cell Sci.* **108**, 2301 (1995).
16. C. D. Van Raamsdonk, K. R. Fitch, H. Fuchs, M. H. de Angelis, G. S. Barsh, *Nat. Genet.* **36**, 961 (2004).
17. C. D. Van Raamsdonk, G. S. Barsh, K. Wakamatsu, S. Ito, *Pigment Cell Melanoma Res.* **22**, 819 (2009).
18. R. J. Garcia *et al.*, *J. Invest. Dermatol.* **128**, 131 (2008).
19. A. Nakamasu, G. Takahashi, A. Kanbe, S. Kondo, *Proc. Natl. Acad. Sci. U.S.A.* **106**, 8429 (2009).
20. M. Iwashita *et al.*, *PLoS Genet.* **2**, e197 (2006).
21. M. Watanabe *et al.*, *EMBO Rep.* **7**, 893 (2006).

Acknowledgments: We thank San Jose Animal Care and Services, Fix Our Ferals, the Berkeley East-Bay Humane Society, Pets In Need, the Monterey Animal Hospital, and the City of Huntsville Animal Shelter for assistance with sample collection; the Wild Cat Education and Conservation Fund for contributing king cheetah samples; R. Finn for assistance with Norwegian Forest Cat samples and phenotypes; H. Flick for domestic cat photographs; and J. C. Kaelin for help with feral cat sample collection. We thank the Production Sequencing Group of the Washington University School of Medicine Genome Center for cDNA sequencing. Namibian samples were collected with the approval of the Ministry of Environment and Tourism (permit

1532). Supported in part by the HudsonAlpha Institute for Biotechnology and by the Intramural Research Program of the NIH, National Cancer Institute, Center for Cancer Research, using federal funds under contract N01-CO-12400. L.Z.H. and J.P. were supported by fellowships from Genentech and the National Institutes of Health, respectively. A.vD. is the founder and director of the Ann van Dyk Cheetah Centre, a nonprofit conservation organization. DNA sequence data for this study are available at http://genome.wustl.edu/genomes/view/felis_catus/ and the NIH Short Read Archive (SRA056885).

Supplementary Materials
www.sciencemag.org/cgi/content/full/337/6101/1536/DC1
Materials and Methods
Supplementary Text
Tables S1 to S9
Figs. S1 to S7
References (*22*–*36*)

22 February 2012; accepted 20 July 2012
10.1126/science.1220893

Loss of the Tumor Suppressor BAP1 Causes Myeloid Transformation

Anwesha Dey,[1] Dhaya Seshasayee,[2] Rajkumar Noubade,[2] Dorothy M. French,[3] Jinfeng Liu,[4] Mira S. Chaurushiya,[1] Donald S. Kirkpatrick,[5] Victoria C. Pham,[5] Jennie R. Lill,[5] Corey E. Bakalarski,[4] Jiansheng Wu,[5] Lilian Phu,[5] Paula Katavolos,[6] Lindsay M. LaFave,[7] Omar Abdel-Wahab,[7] Zora Modrusan,[8] Somasekar Seshagiri,[8] Ken Dong,[9] Zhonghua Lin,[10] Mercedesz Balazs,[10] Rowena Suriben,[1] Kim Newton,[1] Sarah Hymowitz,[9] Guillermo Garcia-Manero,[11] Flavius Martin,[2] Ross L. Levine,[7] Vishva M. Dixit[1]*

De-ubiquitinating enzyme BAP1 is mutated in a hereditary cancer syndrome with increased risk of mesothelioma and uveal melanoma. Somatic *BAP1* mutations occur in various malignancies. We show that mouse *Bap1* gene deletion is lethal during embryogenesis, but systemic or hematopoietic-restricted deletion in adults recapitulates features of human myelodysplastic syndrome (MDS). Knockin mice expressing BAP1 with a 3xFlag tag revealed that BAP1 interacts with host cell factor–1 (HCF-1), O-linked *N*-acetylglucosamine transferase (OGT), and the polycomb group proteins ASXL1 and ASXL2 in vivo. OGT and HCF-1 levels were decreased by *Bap1* deletion, indicating a critical role for BAP1 in stabilizing these epigenetic regulators. Human *ASXL1* is mutated frequently in chronic myelomonocytic leukemia (CMML) so an ASXL/BAP1 complex may suppress CMML. A *BAP1* catalytic mutation found in a MDS patient implies that BAP1 loss of function has similar consequences in mice and humans.

Somatic inactivating *BAP1* mutations occur in the majority of metastatic uveal melanomas and approximately one-quarter of malignant pleural mesotheliomas. Somatic mutations also have been identified in breast, lung, and renal cell cancers (*1*–*5*). Recently, germline *BAP1* mutations were linked to a tumor predisposition syndrome characterized by melanocytic tumors, mesothelioma, and uveal melanoma (*6*, *7*).

We investigated the normal physiological role of BAP1 using BAP1-deficient mice (fig. S1A). $Bap1^{-/-}$ embryos showed developmental retardation at embryonic day 8.5 (E8.5) and were not detected beyond E9.5, indicating that BAP1 is essential for embryo development (fig. S1, B and C). To bypass this embryonic lethality, we bred mice that expressed the tamoxifen-inducible recombinase creERT2 ubiquitously from the *Rosa26* locus (*8*) and had *Bap1* exons 4 and 5 flanked by lox sites (floxed) (fig. S1A). The floxed *Bap1* exons were deleted from most adult mouse tissues at 1 week after daily tamoxifen injections for 5 days were completed, the brain being the expected exception (fig. S1D). Loss of *Bap1* mRNA from hematopoietic lineages at 1 week after the final tamoxifen injection was confirmed by quantitative reverse transcription polymerase chain reaction (fig. S1E), and BAP1 protein was no longer detected in splenocytes by Western blotting (fig. S1F). Within 4 weeks of the last tamoxifen injection, 100% of the $Bap1^{fl/fl}$ creERT2^{+} mice [hereafter referred to as BAP1 knockout (BAP1 KO) mice] developed splenomegaly (n = 12 mice). This phenotype was never observed in $Bap1^{+/+}$ creERT2^{+} control mice [hereafter referred to as wild-type (WT) mice] (Fig. 1, A and B). Histopathology, flow cytometry, and myeloperoxidase immunohistochemistry revealed that splenomegaly in the KO mice resulted from extramedullary hematopoiesis and expansion of the myeloid lineage (Fig. 1, C to E). Myeloid cells also were increased in lymph nodes (fig. S2) and bone marrow (Fig. 1F).

Peripheral blood taken from 11 out of 12 BAP1 KO mice at 4 weeks after the final tamoxifen injection showed cytological features consistent with myelodysplasia and ineffective erythropoiesis (Fig. 1G). Total leukocyte numbers were elevated (Fig. 1H) because of monocytosis (Fig. 1I) and neutrophilia (Fig. 1J), which is consistent with chronic myelomonocytic leukemia (CMML)–like disease [classified as a myelodysplastic/myeloproliferative disease according to the new World Health Organization classification of myeloid neoplasms (*9*)]. Thrombocytopenia was detected as early as 1 week after the final tamoxifen injection (Fig. 1K), and all diseased mice developed severe progressive anemia (Fig. 1L). We noted morphologic features of erythroid dysplasia, including increased numbers of nucleated red blood cells, anisopoikilocytosis, and prominent basophilic stippling (Fig. 1L). Hypersegmented neutrophils (Fig. 1J), bilobed granulocytes (Fig. 1I), giant platelets (Fig. 1K), hyposegmented neutrophils consistent with pseudo-Pelger-Huët anomaly, and atypical immature cells with myelomonocytic features were also observed. Mitotic figures and apoptotic cells (fig. S3) were consistent with human myelodysplastic syndrome (MDS) (*10*), whereas blasts were rare. Collectively, these data show that *Bap1* deletion produces a myeloproliferative/myelodysplastic disorder with features of human CMML. Consistent with what is seen in patients with end-organ damage from myeloid neoplasms, the BAP1 KO heart contained microthrombi with multifocal necrosis, neutrophilic inflammation, and infiltration of myeloblastic cells (fig. S4).

Given that chronic myeloid neoplasms originate in the phenotypic hematopoietic stem cell (HSC) compartment (*11*), we characterized the lineage-depleted hematopoietic progenitor cell population in the BAP1 KO mice. Lineage-negative Scal^{-} c-Kit^{+} myeloid progenitor cells and HSC-enriched lineage-negative Scal^{+} c-Kit^{+} (LSK) cells were increased in BAP1 KO spleen and bone marrow as early as 2 weeks after the final tamoxifen injection (fig. S5A). Given that BAP1 KO mice develop monocytosis and neutrophilia, BAP1 KO LSK cells harvested 1 month after tamoxifen treatment expressed higher levels of a subset of genes involved in myelopoiesis [fig. S5, B and C (*12*)]. In methylcellulose colony-forming assays, BAP1 KO LSK cells yielded fewer colonies than WT LSK cells (fig. S6, A and B). In addition, unlike cells from WT colonies, which could be replated after 10 days in culture to form new colonies, replated BAP1 KO cells did not produce well-formed colonies, and many exhibited cytoplasmic blebbing characteristic of apoptosis (fig. S6, C and D). These in vitro data suggest that BAP1

[1]Department of Physiological Chemistry, Genentech, 1 DNA Way, South San Francisco, CA 94080, USA. [2]Department of Immunology, Genentech, 1 DNA Way, South San Francisco, CA 94080, USA. [3]Department of Pathology, Genentech, 1 DNA Way, South San Francisco, CA 94080, USA. [4]Department of Bioinformatics and Computational Biology, Genentech, 1 DNA Way, South San Francisco, CA 94080, USA. [5]Department of Protein Chemistry, Genentech, 1 DNA Way, South San Francisco, CA 94080, USA. [6]Department of Safety Assessment, Genentech, 1 DNA Way, South San Francisco, CA 94080, USA. [7]Human Oncology and Pathogenesis Program and Leukemia Service, Memorial Sloan-Kettering Cancer Center, 1275 York Avenue, New York, NY 10065, USA. [8]Department of Molecular Biology, Genentech, 1 DNA Way, South San Francisco, CA 94080, USA. [9]Department of Structural Biology, Genentech, 1 DNA Way, South San Francisco, CA 94080, USA. [10]Department of Translational Immunology, Genentech, 1 DNA Way, South San Francisco, CA 94080, USA. [11]MD Anderson Cancer Center, 1515 Holcombe Boulevard, Houston, TX 77030, USA.

*To whom correspondence should be addressed. E-mail: dixit@gene.com

www.sciencemag.org/cgi/content/full/337/6101/1536/DC1

Supplementary Materials for

Specifying and Sustaining Pigmentation Patterns in Domestic and Wild Cats

Christopher B. Kaelin, Xiao Xu, Lewis Z. Hong, Victor A. David, Kelly A. McGowan, Anne Schmidt-Küntzel, Melody E. Roelke, Javier Pino, Joan Pontius, Gregory M. Cooper, Hermogenes Manuel, William F. Swanson, Laurie Marker, Cindy K. Harper, Ann van Dyk, Bisong Yue, James C. Mullikin, Wesley C. Warren, Eduardo Eizirik, Lidia Kos, Stephen J. O'Brien,* Gregory S. Barsh,* Marilyn Menotti-Raymond

*To whom correspondence and requests for materials should be addressed. E-mail: gbarsh@hudsonalpha.org (G.S.B.); lgdchief@gmail.com (S.J.O'B.).

Published 21 September 2012, *Science* **337**, 1536 (2012)
DOI: 10.1126/science.1220893

This PDF file includes:

Supplementary materials:

Materials and Methods

Biological samples

DNA samples and phenotype information from outbred and/or feral cats were collected at five spay/neuter clinics in Northern California. Additional domestic cat DNA samples including breed cats and a research pedigree at the NIH, as well as some cheetah DNA samples, were from a collection maintained at the Laboratory for Genomic Diversity, NCI-Frederick, MD. Samples from the Laboratory of Genomic Diversity were collected in full compliance with specific Federal Fish and Wildlife permits from the Conservation of International Trade in Endangered Species of Wild flora and Fauna: Endangered and Threatened Species, Captive Bred issued to the National Cancer Institute (NCI)-National Institutes of Health (NIH) (S.J.O. principal officer) by the U.S. Fish and Wildlife Services of the Department of the Interior. DNA from the index king cheetah (individual #4 in Fig. S3) was collected from the Wild Cat Conservation and Education Fund in Occidental, California, and studied at Stanford University; DNA samples from the remaining individuals in the captive cheetah pedigree (Fig. S3) were collected at the Ann van Dyk Cheetah Centre from blood samples obtained during routine veterinary examinations, and studied at the University of Pretoria.

For analysis of gene expression in cheetah skin, 4 mm biopsy punches from animals at the Cheetah Conservation Fund (Otjiwarongo, Namibia) were obtained when animals were under general anesthesia during routine veterinary examinations. For histological and gene expression studies of domestic cats, tissue samples from fetal and newborn animals were obtained from the City of Huntsville Animal Shelter from animals that had been euthanized for reasons unrelated to this study.

For studies of *Edn3* expression in the skin of transgenic mice, we made use of a previously described *TRE::Edn3* transgenic line in which expression of *Edn3* requires the presence of a second transgene, *K5::tTA* (*18*). The original description of these animals focused mainly on pigment cell development, documented a very strong effect of the transgene on the accumulation of melanocytes in the fetal dermis, and included one panel showing that the transgene caused darkening of an A^y coat. For analysis of gene expression in these mice, tissues were prepared from animals on a mixed FVB/N, C57BL/6J background; no differences were observed between A^y/-; +/+ animals and A^y/*a*; *Tg.K5-tTA* animals. For analysis of gene expression during mouse development, tissues were prepared from FVB/N animals. All work in mice, cats, and cheetahs was carried out under animal protocols approved by local institutional review boards.

SNP discovery and genome sequences

Genomic DNA isolated from a pedigreed Ta^M/Ta^b cat was amplified using 111 primer sets (Table S3), chosen to amplify potential exons based on comparative mapping (Fig. 1B). Sheared PCR amplicons were sequenced on an Illumina Genome Analyzer IIx. Mapping and Assembly with Qualities (*22*) was used to map sequencing reads to a concatenated reference encompassing all amplicon sequences and to determine heterozygous base positions, as indicated in Table S4.

Primer sets for SNP discovery were designed based on the 1.9x *Felis catus* genome assembly (felCat3, v12.2) (*23*). While this work was underway, a 3x assembly (felCat4) (*24*) and some

information from an ~10x assembly became available (*25*), and was used to design additional primer sets as described in Tables S3 and S4.

Linkage, association and haplotype mapping

Initial linkage studies are described in ref. (*7*); we used information from the 3x genome assembly together with an integrated microsatellite and comparative map (*23*, *26*, *27*) to define the linkage intervals depicted in Fig. 1B. For association mapping in feral cats from Northern California, we initially genotyped 58 SNPs in 8 blotched and 9 mackerel cats, then expanded the sample set to include 16 blotched and 33 mackerel cats for a subset of those SNPs in a second stage (Fig. S1). Initial haplotypes were based on 23 SNPs genotyped in 58 blotched and 19 mackerel cats from the feral cat population in Northern California. Three additional *Tabby* alleles (S59X, T139N, D228N; SNPs "S", "Q", and "P", respectively, Table S3) were discovered by resequencing *Taqpep* exons (Table S4), leading to an expanded set of haplotypes based on 26 SNPs genotyped in 58 blotched, 19 mackerel, and 4 "atypical swirled" cats from the feral population in Northern California (Fig. S2A, S2B, S2C) and 3 blotched and 3 mackerel cats from the NIH colony (Fig. S2D). Genotyping was carried out by capillary-based sequencing; the call rate at each stage (proportion of samples for which an accurate genotype could be inferred) was >95%. Association results (Fig. S1) were evaluated by comparing allele counts from blotched and mackerel cats in a 2x2 contingency table using a Bonferroni-corrected chi-square test (with 1 degree of freedom). Haplotypes were inferred with PHASE v2.1 (*28*). Primer sets and amplicons are described in Tables S3, S4, and S5.

Cheetah genetics

Cheetahs were surveyed for the presence of the *N977Kfs110* allele with 'Exon20c' primer set from Table S4. To test for linkage with the king cheetah phenotype, genotype results for 31 members of a multi-generational captive bred pedigree maintained at the Ann van Dyk Cheetah Center were analyzed with SUPERLINK v1.7 (*29*) under a model of recessive inheritance.

Phylogenetic analysis

To assess the phylogenetic history of *Taqpep* in felids and other mammals, we manually generated an alignment including orthologs from 31 felid species (all of which had identical length proteins), and manually merged this alignment to the *Taqpep* alignment for 23 non-felid mammals (most distant species was platypus) extracted from the 44-way whole-genome vertebrate sequence alignments (http://genome.ucsc.edu). The latter alignment included 23 mammals after removal of non-mammalian vertebrate sequences and any sequence with more than 500 gap characters (the total alignment length was 2,976 nucleotides or 992 codons). The alignment was further projected to a 'felid' frame in which gaps in the felid species were eliminated. A total of three stop codons in two of the 23 non-felid mammalian species were assumed to represent sequence errors and manually changed to gap characters prior to analysis since each of these species exhibited high-quality full-length protein alignments except for the stop codons.

We used MAPP (*12*) to estimate the functional impact of felid-specific amino acid substitutions. Briefly, MAPP quantifies rates of evolution in biochemical terms (*e.g.* amino acid size or polarity) in a group of aligned proteins; the diversity within this alignment is considered to represent the range of

variation compatible with protein function. Functional effects of all substitutions are then estimated on the basis of the phylogenetically weighted biochemical distance between the mutant residue and the aligned sequences. To generate MAPP scores (*12*), we used the felid-projected alignment of the 23 non-felid mammalian *Taqpep* sequences; this allows unbiased estimation of the effects of potentially deleterious, or other change of function, substitutions observed specifically in cats, *i.e.*, if felids were included in MAPP scoring, these substitutions would tend to be considered acceptable and have reduced scores.

Gene expression profiling (EDGE) of cheetah skin

Cheetah skin biopsies were obtained from a black-colored spot and an adjacent yellow-colored background region and preserved in RNAlater (Ambion Life Technologies, Grand Island, NY). Following the isolation of total RNA using a commercial kit (RNeasy Fibrous Tissue Mini kit, Qiagen, Valencia, CA), EDGE libraries were constructed from five pairs of cheetah samples and each library was sequenced on one lane of an Illumina Genome Analyzer IIx. For gene expression profiling, the EDGE protocol and preliminary results obtained with a single animal (that is also included as 1 of the 5 animals presented here) are described in Hong et al. (*13*). In that work, EDGE tags were assigned to genes using the 1.9x assembly (felCat3, v12.2) and a partial transcriptome from the domestic cat. For the work described here, we also used information from an ~10x assembly (*25*).

Differentially expressed genes were identified using an overdispersed Poisson model implemented in the edgeR package (*30*). We carried out a paired analysis by estimating the dispersion parameter using an empirical Bayes method that depends on the overall expression level for each gene. The adjusted gene counts are fit to a negative binomial generalized linear model, and the results are then analyzed with a likelihood ratio test. P values were adjusted for multiple testing using the false discovery rate correction (*31*), and an FDR cutoff of 5% was used to identify differentially expressed genes.

qPCR-based measurements of mRNA levels

Total RNA for qRT-PCR was isolated using Trizol (Invitrogen Life Technologies, Grand Island, NY), purified using RNeasy (Qiagen), and treated with DNaseI (Invitrogen) before reverse transcription with Superscript III (Invitrogen). cDNA was amplified using the LightCycler FastStart DNA Master Plus Sybr Green I System (Roche Diagnostics, Indianapolis, IN). *Bactin* or *Gapdh* were used to compare relative levels of mRNA between different tissues and developmental stages in the mouse (Fig. S6) or between different regions of felid skin (Fig. 4C). Primer sequences are given in Table S9.

In situ hybridization

Digoxigenin-labeled RNA probes were generated from the 3'UTR of mouse and cat *Taqpep* and cat *Edn3* using in vitro transcription (Roche Diagnostics) and a PCR-generated template. Primer sequences are described in Table S9. Prior to embedding, E17.5 mouse embryos, postnatal day 7 mouse dorsal skin, and fetal cat skin was fixed in 4% paraformaldehyde followed by 30% sucrose for 24 hours. Frozen sections (12um) were cut and mounted on Superfrost Plus slides (Fisher

Scientific, Pittsburgh, PA). Sections were fixed with 4% paraformaldehyde for 10 minutes, treated with proteinase K (Sigma, St. Louis, MO), hybridized overnight at 60 degrees, incubated with alkaline phosphatase-conjugated anti-digoxigenin antibody (Roche Diagnostics) overnight at 4 degrees and developed 3-6 hours in a buffer containing BCIP/NBT substrate (Roche Diagnostics). Results depicted in Fig. 4C (*Edn3* in cat dermal papilla) were repeated at least 3 times.

Morphometric analysis of cheetah skin

Skin biopsies from black- and yellow-colored areas of 3 individuals were examined, recording 10 high-power fields for each sample, and measuring with ImageJ (*32*) the width of complex follicle clusters, the inter-cluster distance, and the density of pigmented cells in the interfollicular epidermis (Fig. S5A, S5B).

Author contributions

C.B.K. collected the feral cats, carried out the association and haplotype studies, identified the index king cheetah mutation, and coordinated the project. X.X. helped with the association analysis and carried out the sequence analysis of *Taqpep* in breed cats and other felid species as part of a graduate program supervised by B.Y. Gene expression profiling and mouse *Taqpep* expression studies were carried out by L.Z.H. and K.A.M., respectively. V.A.D. carried out the cheetah genotyping and linkage analysis, with support from C.K.H. and A.v.D. The cheetah and leopard skin biopsies were collected by A.S.-K. with the support of L.M., several *F. nigripes* samples were provided by W.F.S, and M.E.R. helped with the collection and analysis of breed cats and cat tissue samples. J. Pontius and H.M. provided bioinformatic and technical support, respectively. G.M.C. carried out the MAPP analysis with input from C.B.K., E.E., and G.S.B. J. Pino and L.K. generated *Edn3* transgenic mice; production of the cat transcriptome and genome assembly was supervised by J.C.M. and W.C.W. Linkage studies for tabby were initiated by E.E. with support from S.J.O., who developed this research initially as leader of the Laboratory for Genomic Diversity. G.S.B. and M.M.-R. coordinated and led the project; G.S.B., C.B.K and M.M.-R. wrote the manuscript with input from V.A.D., A.S.-K., E.E., and S.J.O.

Competing interest statement

The content of this publication does not necessarily reflect the views or policies of the Department of Health and Human Services, nor does its mention of trade names, commercial products, or organizations imply endorsement by the U.S. Government. The funders had no role in study design, data collection and analysis, decision to publish, or preparation of manuscript.

Table S1: Survey of genotype/phenotype correlation in feral cats[a]

	Blotched	Mackerel	Atypical Swirled
S59X/W841X	4	0	0
W841X/W841X	54	0	0
S59X/T139N	0	0	1
W841X/T139N	0	7	3
T139N/T139N	0	2	0
Total	58	9	4
S59X/+	0	2	0
W841X/+	0	26	0
T139N/+	0	5	0
+/+	0	9	0
Total	0	42	0

[a] Feral cats from Northern California spay/neuter clinics. The phenotypes of Blotched, Mackerel, or Atypical Swirled are illustrated in Fig. 1 and Fig. S4. Haplotypes for the 58 blotched cats and 19 of the mackerel cats are shown in Fig. S2. An additional *Ta*^{b} allele, D228N, was observed in an NIH colony (Fig. S2).

Table S2. Distribution of *Taqpep* alleles among breed cats

Domestic cat breeds (n)	Geographic origin	Allele Frequency			
		S59X	A/T139N	D228N[a]	W841X
American Curl (4)	Western	0	0	0	0.38
Abyssinian (8)	Western	0	0	0	1
American Shorthair (25)	Western	0.08	0	0	0.82
American Wirehair (8)	Western	0	0	0	0.81
Bengal (16)	Western	0	0.03	0	0.50
Chartreux (11)	Western	0	0	0	0.55
Cornish Rex (20)	Western	0	0	0	0.30
Devon Rex (20)	Western	0	0	0	0.13
Egyptian Mau (14)	Western	0	0.11	0	0.21
Exotic Shorthair (18)	Western	0	0.03	0	0.78
Himalayan (15)	Western	0	0.03	0	0.77
Manx (17)	Western	0	0	0	0.79
Munchkin (15)	Western	0	0.23	0	0.47
Norwegian Forest Cat (12)[b]	Western	0.29	0	0	0.21
Ocicat (16)	Western	0	0.19	0	0.41
Persian (20)	Western	0	0.10	0	0.68
Scottish fold (17)	Western	0	0	0	0.65
Selkirk Rex (16)	Western	0	0	0	0.56
Sphynx (18)	Western	0	0	0	0.11
Turkish Van (8)	Western	0	0	0	0.50
Birman (12)	Eastern[c]	0	0	0	0.71
Bobtail (14)	Eastern	0	0.18	0	0.04
Burmese (12)	Eastern	0	0	0	0
Siamese (15)	Eastern	0	0	0	0.20
Total (351)		0.015	0.04	0	0.48

[a] Mutation observed in NIH animal colony, but not in breed survey.

[b] Among 12 Norwegian Forest Cats, 1 homozygote and 5 heterozygotes or compound heterozygotes were observed for S59X.

[c] Although the Birman breed is said to have an Eastern origin, the breed underwent a severe bottleneck in the 1940s and was outcrossed extensively to Western breeds.

Table S3. Amplicons for *Tabby* candidate region exon sequencing[a]

Amplicon	Size(bp)	Forward primer	Reverse primer
TaExon-Un11-1	460	TCAGGTTCTCTCTGGCCACT	CAGGTGCCCCTAAAGTGATT
TaExon-Un11-2	482	ATCTGCCCACAGCCTTAGTG	TGACAAGGGTCTATTTGGCA
TaExon-Un11-3	2000	TCCAGTTCTCGGTTTTGGTAA	CCGTCATGGGCATAATTTTT
TaExon-Un11-4	470	TTTCAGATACTAACAGTGCCTTTTT	ACCCTTAGCACCCAACAGTG
TaExon-Un11-5	987	ATGGTTCTTTGCTGGTTTGG	AGCATGCACTAGGAGAGTTGC
TaExon-Un11-6	1802	GTTCAATGCCATGTGTGAGG	AGGTGCAGTAATGGATTGGC
TaExon-Un11-7	593	GGCAACACAATTTTAATCATGG	GAAAATGAGAGAATCAGTTTGCTTT
TaExon-Un11-8	602	TACGTGAGTGCCTTGTGAGG	AGCCTGGCCTACAACCCTAA
TaExon-Un11-9	575	GCGTTTGCTGTGATGAAATC	TAGGCGCCCCCTTAAGAATA
TaExon-Un11-10	575	GCGTTTGCTGTGATGAAATC	TAGGCGCCCCCTTAAGAATA
TaExon-Un11-11	617	TGGGACAGTGATAACGATGAAG	TTCAACTGGCCACTGTGTAACT
TaExon-Un11-12	537	TGGGTCATGAATTCTTTTGCT	GACCGCGTGAGACTAGAAGG
TaExon-Un11-13	591	CGTGGCAAACATTATATTGGG	GGGGCTGACAAGAGCATAAG
TaExon-Un11-14	485	TGCACGTTTACACTCAAAGGA	TGCCAAATGTACTTTTTCCTCA
TaExon-Un11-15	628	CCTCCAAACTACCCTCCTCC	GCCCCAACAATGCTTTTATT
TaExon-Un11-16	671	AAATGTGAAATCGGAAGTGTCA	TAATCCAAAAGCACTGGGAA
TaExon-Un11-17	603	CTGCAGAAGACAAATGTGGG	ACGAGCCAAGAACTGCAAAT
TaExon-Un11-18	456	TTCACAGGTTGGGTGTTTTG	TCCAGGAACATTTTTGGAACA
TaExon-Un11-19	608	TCCTGTCTCATTAGGTGAGTCTTTT	GGCGCCCTCTCTTTTAAATAC
TaExon-Un11-20	517	TGGGGGTTAAGAGCTGAAGA	GCTTGCTGAGGACTGATGTG
TaExon-Un11-21	635	CAGATATCTCAGTGTTTGTGCATT	TCACTGGTGCAGGAGTATCG
TaExon-Un11-22	614	TCTTGGGTTTCTCTGACCTACC	CACTGGAAACAAAGTCCGGT
TaExon-Un11-23	544	CCACCAGCAATTTGGGTAAT	AAAAAGCAACAGGCACAAAAA
TaExon-Un11-24	632	TTTTGCACCGTTATGTCGAA	AGGGGAGGGAAAGGATAAGG
TaExon-Un11-25	600	TTCTTCTGCTGGGCAAGTTT	GGCAACAGTTTCTTGAGGTG
TaExon-Un11-26	531	TTCGTGGGCTGATATGTGTC	TGGCAATCATGACAACTCAAA
TaExon-Un11-27	495	CCTCCAAACTACCCTCCTCC	GCTGCTTTACGCCATCTCTC
TaExon-Un11-28	642	CTGTGACAATTTTCCCTGCAT	ATGTCAACCGGAATGAAAGC
TaExon-Un11-29	630	GGCATGTTCTAGAATTGTGACCT	AAACCACATCCCGATTTGTC
TaExon-Un11-30	642	TGGATGCTGAACTAACGCAG	GCGATTTTGGAAGGAAGTGA
TaExon-Un11-31	635	TCCAAGTCTTCTGTGCACCTT	GCAGGCCAAGGATTATCTGA
TaExon-Un11-32	946	GCTGCCCACTCTTATACCCA	GTTCAAACCACATCCCGATT
TaExon-A1-1	648	ACAAAGTCCAAAATCCGTGC	TGTCTCCTTTGTAGATGATAGGTTTG
TaExon-A1-2	547	GGGGGAAAAATGGAACAGAT	TCAGCAAGTTGCCCCTTTAC
TaExon-A1-3	463	GCTGATAATTGAGCTTGGGC	ACACATAGTTGGAGGCAGGG
TaExon-A1-4	496	ATTCAGAGGCTGCTTGCATT	CTAGGATTCCTGCTTGGCTG
TaExon-A1-5	505	GATACATGGGGAAGGAGGGT	CAGAACAGCCATCTCACCAA
TaExon-A1-6	588	AGCCCCTAACTCCCCTACAA	CCAGTGTTGCAAGCCAAAAT
TaExon-A1-7	648	CCTCCAGAAAGATCCCATGA	TACGGCTGGAGATAACCGTC
TaExon-A1-8	608	CCCAATGTCTAATGGCCCTA	ACTTTGGCCGAGTCTTCTCA
TaExon-A1-9	493	CAGCAATGCACTCTGCAAAT	CTCCCAAGACCTGTGACCAT
TaExon-A1-10	492	CCTCTCTGCCGAGAACTTTG	TATGCCCCTTTCAGATCAGC
TaExon-A1-11	541	ATGTTTAGGAGGTTTGGGGC	TGTGGATGGGGGAAAGTAAA
TaExon-A1-12	478	CTTGGAAGGGAATGTGTTGC	TGGCTGAACAAAACGTGGTA
TaExon-A1-13	451	TTTTCAATGCATGATTTTTATCG	CAGGCGCCCCTAGTTTATTT
TaExon-A1-14	645	CCATCATGGGGAAATTTGTT	TTCACAGTGGTCTCCACCAA
TaExon-A1-15	462	GCAGCTGCCAGAATAAAAGG	CCATAAGCGAACCGTGTTTT
TaExon-A1-16	539	ACCCCGTTCACCTCTTTTCT	TTTGTACGCATCTCCTCGTG
TaExon-A1-17	769	CATTTTGACGTGCTCATTGG	CCGGATTCAGGAACCCTATT
TaExon-A1-18	486	GAGAGCCGTTGGTACAGTCC	CACGAAGAGGACAAAACCCT
TaExon-A1-19	573	CTCAAGAACTTCCAGCAGGG	GCATGGGACAGAGTAGGGAA
TaExon-A1-20	640	GCAAGCAAGCTAAATGAGCC	GTGGAAGAGGATTTCCCACA
TaExon-A1-21	450	CCCACTCTGCCCAAGATAAA	AATGTTTGCCCTCTCGTGAC
TaExon-A1-22	1985	AGATTCAACCCTCATGCTGC	GAGTGGGGTGAATGGAAGAA
TaExon-A1-23	1000	GAATTCGTACATGGCGGAGT	ATGGTGAAAAGGGGGATTTC
TaExon-A1-24	643	CACCCAGAATCCTGAGGAAA	GCCCCGAAGATCACCTACTA
TaExon-A1-25	577	ACCTTCATGCCTTCATGGTC	GCATGCAGTACCACATACGG

TaExon-A1-26	587	CCAGAAGCGACTGCATGTTA	CCCAAAGCGCTTAAACTCAG
TaExon-A1-27	464	ATGCCTGGTTTCTCCTTCCT	CGCTGTTCCCTTGATTTGAT
TaExon-A1-28	491	CCTCCAGAAAGATCCCATGA	TTAGAGTCCAGGGGTGGTTG
TaExon-A1-29	936	AGGAAGAAGTGAAGCCCTCC	AAACAACATCGCAAAGGACC
TaExon-A1-30	470	CCTCGCAATCCAAGGTTTTA	TCACGACTCCATGATCCAAA
TaExon-A1-31	480	TGCTCGAACTACCCCTTTGT	CTTGAGAAATCACCCCAGGA
TaExon-A1-32	1665	TTCTGGGGATAGTTGATGGC	GGCCTAAGATTTTGGTGGGT
TaExon-A1-33	890	GAAGGCACAGGTGAGTGAGG	GCGTCCCAGAATGTAGCAGT
TaExon-A1-34	481	AGGGATCTCACCCACTAGTCC	TCATCAACTGAGTATCAACTTCATT
TaExon-A1-35	611	GGGCACCTTTTACTTCACCA	TTGGGCACTTGAATGTACCA
TaExon-A1-36	484	TTCCCTGAAGCTTTAGATTTGC	TCCAGCTGAACAGCTCTCAA
TaExon-A1-37	644	TCCCCACACATACGTTCTCA	TGTTCATTGTCTGGGACCAA
TaExon-A1-38	608	CCCCAAGCCTGTTGTTTTTA	GCCAGAGTTTCCGAAAGTGA
TaExon-A1-39	578	GCGCCATAATAGGGCATTTA	GCTGTCGTGTTAATTGCGAA
TaExon-A1-40	475	GTCAAACCCAGGATGCAGTT	GCTCTTTGGAAGGCGTTATG
TaExon-A1-41	453	TGATTCTCAAAACCTGTCACAAA	ATGAGCCCAAAGGGAGAGTT
TaExon-A1-42	618	AAGATGTTGGCAGCCTGTTT	TTGGCAAAGGATTCTGCTCT
TaExon-A1-43	949	TCCTTGGTGTTTCCATCACA	CCCACGTAGCACAAAACCTT
TaExon-A1-44	590	CCTCTGAACAGGGGACAAAA	GGGAAAAGGTTTAAGCTGGG
TaExon-A1-45	1957	TCGTGACGCTCATCAAAGAC	GGCTACTCTGAACACCCAGC
TaExon-A1-46	603	CAGCACAGGCTCAGATACCA	GGGGATAGGGACAGAAGACC
TaExon-A1-47	540	TTCCAAATACATGGGGCAAT	GCTGGGTTGTTTTCTGTGGT
TaExon-A1-48	485	GCACAGTGCTTAGAGGGGAG	ATTGGTACCCTCCTGCTCCT
TaExon-A1-49	894	AAACTCACAAATCCTCCCCC	CAATGTGGGATGACTCAACG
TaExon-A1-50	620	ACATGGAACCTGAGTCCCAA	GCTGGCCATCATCTGTTTTT
TaExon-A1-51	632	GAAATCGGACCCAGTACGAA	ACCGAATTCCCTAAGGTTGG
TaExon-A1-52	557	CCAATTGGGGATTCAGTTTG	GCAAACCCACATCAATTTCC
TaExon-A1-53	607	CCTGGACCTGTGGAAAGAAA	TCCTTCCGTTTCCCACTAAA
TaExon-A1-54	1508	ACTCTCACCATCCACCCAAG	ACACACACACACACACACGG
TaExon-A1-55	787	TGATGGCAAATCGTCTTCTG	CCTTGAGTTCCTGGTTGCTC
TaExon-A1-56	641	GGGGCATTATGTGTTCATCTG	TGCCTTAGTTCTGTGTTTCCTG
TaExon-A1-57	624	CCATTTGAAAATGCCTCCAT	CTGTCTGTATGGCCAGGGAT
TaExon-A1-58	558	GGTCAGCATCACCTTTTGGT	TGCCTATGGGAAAGTCTGCT
TaExon-A1-59	593	CTTGGCCAGGATAGGAAACA	CCTCTAAGCACTGTGCCCTC
TaExon-A1-60	486	AGCTGATCCCCTGAAGGATT	AAGGACGGATTAGGTCAGCA
TaExon-A1-61	618	CGGATTCAAAGCAAAGTCAA	TCTGCAAACTTTCCTGCTGA
TaExon-A1-62	933	CAAGGACACCATATGGCAAA	CCCTTTGATGAGGGAGAACA
TaExon-A1-63	1000	TGTCATCTCCCACCTCAGTTC	ACCATCCCATACCAATTCCA
TaExon-A1-64	621	CCCCAAGGAAGGTGAGTACA	TGCACTCAAGGTGAGTTTGC
TaExon-A1-65	474	CTGTTCTTTCTCAGGCCGAC	GCCGGGGGTATAATTTAGGA
TaExon-A1-66	493	CAACAATGCCCATTCCTTCT	TGCGCATCCAAAATTATTCA
TaExon-A1-67	613	TCAACTTGGGCCAGATTTTC	CTGCCCTCCCTTCACATTTA
TaExon-A1-68	572	GCTCTTCAGCTGGAAAATGG	TTCAGCGTTCATCCCTTTCT
TaExon-A1-69	479	CACAGTGGGGAAACTGAGGT	ATTTGTGCGCTGACTCAGAA
TaExon-A1-70	549	TCCACTGTATCCATGGAATTTG	AGCGCTGATTCTGAAATGCT
TaExon-A1-71	460	TGCTTCTTAAAACTGCTTGCTG	CTTGTCTCCAGGTTGGGATG
TaExon-A1-72	644	TGTTTGAAGTGGAAAAGGGG	GAGAGCTGCTGGCTTTGTCT
TaExon-A1-73	567	TGTTTGTTACCCAAGGCAGTT	GCGCCCCTTCTTTCTTTTT
TaExon-A1-74	609	GCAGAGGGAACAGCATCAAT	TGTGAAATGGCAGAATTCAAAC
TaExon-A1-75	506	TCACAAGTGAAGGCATTGGA	TTGCTCAGAATAGACGGGCT
TaExon-A1-76	602	CCCACCCTGCAAGAAAATAA	TTACTGGCAGATATGGGGCT
TaExon-A1-77	611	TGCTGGGATTTAACCAAAGG	AATCCTCCAGAGCAGATTCG
TaExon-A1-78	580	AGAGGGCAGCCTGACTTGTA	AGCCTCAATCAAACGCTCAG
TaExon-A1-79	530	CTCTTGCAACAACATGATGGA	CCATCCCATACCAATTCCAA

[a] Primers were designed for 32 exons from chrUn11 and 79 exons from chrA1 based on annotation of the felCat3 assembly

Table S4. Amplicons for *Tabby* region association and haplotype analysis

Amp.	Size	Forward primer	Reverse primer	SNPs[a,b]
TA-1	373	TGAGAAGAGTGGGCCTTTTG	CCTGAGCCTCTATCATCCCA	3 (3062995,3063104,3063115)
TA-2	365	TGGTTTGGTTCTTAGATAAACATCA T	TGGGGCGTTGTGACATATAC	4 (3067830,3067832,3067957,3067991)
TA-3	361	GAATAGCAGAAATTGCATAAGGC	TCAATAAGCAGAAGCATCTTTCA	3 (3074763,3074824,3074911)
TA-4	347	TACGTGAGTGCCTTGTGAGG	AGGTGCAGTAATGGATTGGC	2 (3077707,3077733)
TA-5	393	GCAGTGATGGAGAGACCGTT	TTCACATGACTCCTCATTCCA	3 (3098108,3098291,3098311)
TA-6	397	TGCAATTCTCCGCCATAAAG	CTGCAAATTAGACACAGAAGGC	6 (3099360,3099444,3099501,3099534,3099537,3099584)
TA-7	397	AGATCCAAACACCATCTGGC	TGACAACTCAAAGCACACCA	1 (3100437)
TA-8	358	TTGCTCAAGCCATGATGTTC	TCTTCAGCTCTTAACCCCCA	1 (3104664)
TA-9	345	AGCTGTGCAAGGTACAACCC	GCTTGCTGAGGACTGATGTG	1 (3105186)
TA-10	374	GAAGGGAGGAAGTTTTCCCA	GAATTCATCCCCGAAAGGTT	1 (120845010)
TA-11	277	GGTGGAAATGGCATCTTTTG	TTTGTACGCATCTCCTCGTG	2 (120853237,120853241)
TA-12	368	GGCTGGAGAAACCAAATTCA	CGTGCAGCTTGGAAAACATA	2 (120858757,120858904)
TA-13	281	CTCTATGGAATGAGGAGGCG	GGGTGCGTTTTGATGAAGTT	1 (120861377)
TA-14	398	GCAAGCAAGCTAAATGAGCC	TTCGTACTGGGTCCGATTTC	1 (120875097)
TA-15	261	CGCCAGTAAGGAGTGAGAGG	AGAAAAGGGGCTGAGAAACC	1 (120889838)
TA-16	267	TCACTCCCAGCTGTAACACG	ATGAGCCCAAAGGGAGAGTT	*2 (A:121238539,B:121238572)*
TA-17	336	TTTCTTTTGCCAGACTGCCT	TGAGTATAATTCAAGGGATCTGTCTG	*1 (C:121262789)*
TA-18	336	AGGAGCCCCAAAAGCATTAT	TGTCCTAGGGAACACAGGCT	*1 (D:121298806)*
TA-19	271	CCCCAAGCCTGTTGTTTTTA	TCAATAGGGGCTGTACGCTT	*1 (E:121344960)*
TA-20	492	CCTCTCTGCCGAGAACTTTG	TATGCCCCTTTCAGATCAGC	*2 (F:121355037,G:121355078)*
TA-21	364	GCTGATAATTGAGCTTGGGC	TTTTTGAAACTGCGTGTTGG	*2 (H:121356067,I:121356070)*
TA-22	370	TAGTAGGTGATCTTCGGGGC	TCTTAGGGAGCATCTTTGGC	*1 (J:121370158)*
TA-23	367	ACCCTTGCAGATCCAGAGAA	TCCGTGTTCAACCAGAATGA	*2 (K,L)*
TA-24	363	TCTGAAATGCACCCACTCAA	GCATTTTGAAAGCATTTGGA	*1 (M)*
TA-25	349	GAATCAGGCTGGCAAACATTA	CCATTTCATTCTACTTTGGTAGCC	*1 (N)*
TA-26	344	CCTCTCAAGGAAGCTACAAGGT	AACCAGATCGTGTGTGTTTCTG	*1 (O)*
TA-27	457	CTCGTGCCTCTGCACTATGA	ACTGGGACGCAGGTAGCA	*1 (P)*
TA-28	548	CCTTCCAGCTCTGGCTTCTA	ATGTCGAAAGCGAACCACA	*3 (Q,R,S)*
TA-29		TCATCAGGTTCAGGGTTCTTG	AAAAAGAAAATAAATATCTGAGTCC A	*1 (T)*
TA-30	311	AAGGGACCGGATGAAAGACT	AGCACCTTTCTGTTTGCCTG	*2 (U:121510763,V:121510796)*
TA-31	311	GACCCCTTGGGACTGTATTACT	CCCTGTTCAGAGGGACAGAA	*3 (W:12119320,X:12119332,Y:12119369)*
TA-32	272	TGAAGAAGCCTCTCAGCTGTC	GTGAGTTTTCCTTACGGCCA	*1 (Z:121528106)*
TA-33	346	GCGTTAGATAGGCAGCAAGG	CCAATCAAGGAATCAGGACAG	1 (122232786)
TA-34	319	AAACCCATATTAGATCCACCTGAA	TTCAGCGTTCATCCCTTTCT	2 (122272066,122272069)
TA-35	367	TCCTTGGTGTTTCCATCACA	ACATTCAGGGCAGGATGAAC	1 (122299065)

[a] Chromosome assignment and SNP position are based on *Felis catus* assembly felCat3, v12.2 (coordinates are not provided for amplicons that are not in the assembly). Amplicons TA-1 – TA-9 are from an unassigned contig (Un11); amplicons TA-10 – TA-35 are from chromosome A1. Size is given in bp.

[b] Italicized SNPs were used for haplotype analysis. Letter designations correspond to the SNP column labels in Figure 1c and fig. S2,S3, and S4.

Table S5. Amplicons for *Taqpep* sequencing in domestic cats and cheetahs

Amplicon [a]	Size(bp)	Forward primer	Reverse Primer
Exon1a[b]	548	CCTTCCAGCTCTGGCTTCTA	ATGTCGAAAGCGAACCACA
Exon1b[b]	457	CTCGTGCCTCTGCACTATGA	ACTGGGACGCAGGTAGCA
Exon1c	655	AAACATCCTCGTCGGAAGTG	ATGTCGAAAGCGAACCACA
Exon2	390	ACAAGCCATCATCCCTCAAT	ACCAACACACGGCCTAGAAA
Exon3	313	CTTAGGGGTGCAGAAATCCA	ACCTGTGGCCAGTATGAAGG
Exon4	396	GGCTTTGACTCGAGAGCATC	TGTGTTTGGGAAGGTGTCAA
Exon5	383	TTTTCTGGATTCTGTCTTCGG	CCTTGGTAGAGCTGCTGGAG
Exon6	387	TCAGAGAAATGCACGACTGC	CACACTCGAAACAATGAAATGC
Exon7	363	TCTGAAATGCACCCACTCAA	GCATTTTGAAAGCATTTGGA
Exon8	337	GCAATGAGAGAAAAGCCCAG	CCATTTGAAAATGCCTCCAT
Exon9	308	TGCACTCAAGGTGAGTTTGC	TAGTAGGTGATCTTCGGGGC
Exon10a	333	GCCCCGAAGATCACCTACTA	CCCCAAGGAAGGTGAGTACA
Exon10b	272	TGCTCTTGTGATGATTTTCCA	CAGGCTGCTTTCCATTTGAT
Exon10c	130	AAAGCATAATGGACCGTTGG	TTGTGGGTTAGGAGAGTCTGA
Exon11	367	ACCCTTGCAGATCCAGAGAA	TCCGTGTTCAACCAGAATGA
Exon12	379	TTTTTGTTGGATTTACTGGGTTT	TCCCTGTCTCTCTACCCTTCC
Exon13	381	AGCGCTGATTCTGAAATGCT	GTTAAGCGTCCGACTTCAGC
Exon14	396	TGTTGAGATCAGGCATCGAA	AGCCGTCCCTAAGAAAACCA
Exon15	301	CCAGTGTTGCAAGCCAAAAT	CATGTAGCTCACCAGTCCCA
Exon16	377	TTATTTGGTGCCTGAAAGCC	TGGTGTTGAAACAGGACGAA
Exon17a	385	CCAGGCACCCTGCTAACTAA	TTAACTGACTGAGCCACCCA
Exon17b[b]	220	CTCTCTGCCGAGAACTTTGG	GCATTGCACCTTCTACCTTACA
Exon18	399	GCGCTGACTCAGAACCCTAA	AGCGACCTTCTCTTCCACAA
Exon19	271	TCAATAGGGGCTGTACGCTT	CCCCAAGCCTGTTGTTTTTA
Exon20a	1979	TTGGCCTTCTTCTGGCTAAA	TGGAAGTGGGACTGTCATCA
Exon20b	319	GTTGGAAGAGCACCAGAAGC	CAAAACCCTCAGCCATCACT
Exon20c[b]	688	TTGGCCTTCTTCTGGCTAAA	TGCTTTCCTTGGCTTTTCTG

[a] Some exons were amplified with multiple primer sets due to exon size, amplification difficulties, or sequence variants within primer binding sites.

[b] Primer sets used for amplification and sequencing of the cat and cheetah *Taqpep* mutations are: Exon1a (S59X and T139N), Exon1b (D228N), Exon17b (W841X), and Exon20c (N977Kfs110).

Table S6. Genotype and phenotype frequencies in feral cats[a]

	Blotched[b]	Mackerel[b]	
		Observed	Expected
$Ta^M/\ Ta^M$	0	16	16.6
$Ta^b/\ Ta^M$	0	36	35.4
$Ta^b/\ Ta^b$	31	0	0
Total	31	52(85)	52

[a] Prior phenotype-based studies have reached conflicting conclusions with regard to potential effects of Ta^b on fitness (*33-35*). The genotype distribution data shown here, based on feral cats from Northern California, are consistent with Hardy-Weinberg expectation.

[b] Among 311 individuals, 116 had distinct tabby markings that allowed them to be classified as blotched (n=31) or mackerel (n=85). Assuming Hardy-Weinberg equilibrium and complete penetrance of the Ta^b allele, this distribution (31 Ta^b/Ta^b and 85 Ta^b/Ta^b or Ta^M/Ta^b) predicts a Ta^b allele frequency of 0.517. Of the mackerel cats, 52 were genotyped (Ta^b refers to the S59X (n=2) or the W841X (n=34) mutations). This population partially overlaps the individuals reported in Table S1.

Table S7. Genes upregulated in black spot areas of cheetah skin[a]

Gene	Fold Change	Pathway[b]	P value	FDR
SILV	7.33	Melanogenesis	7.33E-41	1.03E-36
JAKMIP1	28.1		1.10E-34	7.71E-31
TYR	4.92	Melanogenesis	8.22E-23	3.84E-19
TRPM1	14.5	Melanogenesis	4.10E-20	1.44E-16
ENSFCAG00000010136	3.14		5.89E-15	1.38E-11
HBB	2.94		6.86E-13	1.20E-09
NDUFA2	2.99		1.14E-12	1.78E-09
DCT	3.19	Melanogenesis	4.19E-11	5.33E-08
LIMD2	5.21		6.35E-10	6.36E-07
CA8	7.28		3.92E-09	3.66E-06
RPL36AL	2.6		1.11E-08	9.71E-06
TYRP1	3.08	Melanogenesis	2.21E-08	1.72E-05
DYNC1I1	2.55		5.79E-08	4.06E-05
PLXNC1	2.48		8.40E-08	5.61E-05
RPL26L1	2.06		2.13E-07	1.36E-04
CORO1A	1.97		2.62E-07	1.60E-04
EDN3	4.87	Paracrine signaling	3.59E-07	2.10E-04
LTB	3.21		1.37E-06	7.39E-04
SPI1	2.39		1.36E-06	7.39E-04
OSR1	2.32		1.62E-06	8.41E-04
LRRC33	2.38		3.66E-06	1.83E-03
RAB3IL1	1.91		3.82E-06	1.85E-03
ST6GALNAC3	2.75		4.00E-06	1.87E-03
TMEM200B	4.4		7.66E-06	3.32E-03
FOLR2	1.8		7.82E-06	3.32E-03
CLDN5	1.82		1.11E-05	4.57E-03
C16orf38	2.44		1.44E-05	5.77E-03
MLANA	3.43	Melanogenesis	1.55E-05	5.87E-03
NEDD8	2.9		1.51E-05	5.87E-03
SAA3P	1.76		1.69E-05	6.22E-03
SLC24A5	2.72	Melanogenesis	1.74E-05	6.24E-03
DOK1	2.0		2.05E-05	7.00E-03
C1QTNF5	1.72		2.01E-05	7.00E-03
CHTF18	1.85		2.94E-05	9.57E-03
SVEP1	1.71		3.40E-05	1.08E-02
SLC43A1	1.72		4.30E-05	1.31E-02
SERPING1	1.7		4.30E-05	1.31E-02
TRAFD1	1.75		4.96E-05	1.45E-02
STAT4	2.64		6.15E-05	1.72E-02
CD248	1.68		6.36E-05	1.75E-02
SEPT1	2.65		7.22E-05	1.87E-02
MFAP2	1.76		7.22E-05	1.87E-02

LOC729085	1.99	8.87E-05	2.26E-02
ZIC1	3.62	9.43E-05	2.36E-02
CNNM1	3.7	1.02E-04	2.50E-02
CD209	2.72	1.10E-04	2.66E-02
CCL14	1.65	1.18E-04	2.81E-02
ENSFCAG00000002482	6.45	1.24E-04	2.85E-02
COL6A6	6.05	1.26E-04	2.85E-02
CLEC10A	1.67	1.25E-04	2.85E-02
CLEC1A	2.26	1.34E-04	2.90E-02
BDKRB2	1.72	1.34E-04	2.90E-02
LRRN4CL	1.66	1.32E-04	2.90E-02
RBM19	2.4	2.24E-04	4.61E-02
HIST2H2AA4	3.84	2.35E-04	4.72E-02
NAPSA	1.71	2.39E-04	4.72E-02
PLBD2	1.6	2.36E-04	4.72E-02
MUTYH	1.72	2.54E-04	4.94E-02
TPRA1	3.15	2.61E-04	4.98E-02
TSPAN4	1.61	2.63E-04	4.98E-02

[a] Based on a digital gene expression approach (EDGE) as described in Methods. Genes (FDR < 0.05) are listed in order of increasing P values for significance.
[b] Among 60 genes upregulated in skin from the black spot compared to the yellow inter-spot area, seven encode genes involved in melanogenesis and one encodes a paracrine factor that are candidates for eliciting localized differences in hair color.

Table S8. Genes upregulated in yellow inter-spot areas of cheetah skin[a]

Gene	Fold Change	Pathway[b]	P value	FDR
ENSFCAG00000004053	4.52		1.40E-15	3.93E-12
ENSFCAG00000015326	2.83		1.72E-14	3.44E-11
ENSFCAG00000004061	2.38	KRTAP19-7	1.87E-11	2.62E-08
ENSFCAG00000015327	2.32	KRTAP21-1	8.46E-11	9.87E-08
ENSFCAG00000015329	2.23	KRTAP21-2	3.91E-10	4.22E-07
ENSFCAG00000002173	2.11	KRTAP20-2	1.45E-08	1.20E-05
ENSFCAG00000004049	2.08	KRTAP20-1	3.17E-08	2.34E-05
SPINK6	2.03		6.24E-06	2.82E-03
ENSFCAG00000006428	1.72	KRTAP1-3	2.41E-05	8.05E-03
PCP4	1.81		4.82E-05	1.44E-02
MT1L	1.73		5.69E-05	1.63E-02
TMCO4	1.82		7.04E-05	1.87E-02
SDHB	1.62		1.69E-04	3.59E-02
LYG1	2.44		2.04E-04	4.27E-02

[a] Based on a digital gene expression approach (EDGE) as described in Methods. Genes (FDR < 0.05) are listed in order of increasing P values.

[b] Among 14 genes upregulated in skin from the yellow inter-spot compared to the black spot area, six encode keratin-associated proteins based on sequence similarity to the indicated human proteins.

Table S9. Amplicons used for expression studies

Amplicon	Species	Forward primer	Reverse Primer
Pmel[a]	Mouse	GCACCCAACTTGTTGTTCCT	AGAGATGCAAGGACCACAGC
Slc24a5[a]	Mouse	ACATCCTAGTTTGGATGGTCAC	CTGGTATGCTTGTCCCTGCT
Mlana[a]	Mouse	GCACAGACGCTCCTATGTCA	AGCCGATAAGCAGAGCAATC
Tyr[a]	Mouse	AAATCATCAAGCCCAAGAGC	TGCCCCTGACACTATCACAC
Trpm1[a]	Mouse	GCCTCCTAGCTTTCACATGC	AAGGAGGGGAGGACAGACAT
Edn3[a]	Mouse	AGGCCTGTGCACACTTCTGT	CAGTCTCCCGCATCTCTTCT
Dct[a]	Mouse	GCGTGCTGAACAAGGAATG	CCAGGGTCTGGTGTCTGTTT
Tyrp1[a]	Mouse	TGCTCCAGACAATCTGGGATA	AACGCAGCCACTACAGCAAT
Slc7a11[a]	Mouse	GGCACCTTTGTTCTGGTGAT	ACGTGAGGAACGCAGAGAAC
Bact[a]	Mouse	CGAGCACAGCTTCTTTGCAG	GCAGCGATATCGTCATCCAT
Taqpep[b]	Mouse	CTGAAGTTGGCCGGTACATT	CCCTGGCAATTCTCTTCTTG
Edn3[c]	Cat	ATCTCTGGGAGGCCTCAGTT	GTCCTCAACTCCTGCAAAGC
Edn3[d]	Cat	GGGGAAATTTAAGGTGGTGAA	TCCGGGTGATAGGTACTCCTT
Gapdh[d]	Cat	AAGGTCATCCCAGAGCTGAAT	AGATCCACGACGGACACATT
Pmel[d]	Cat	AGGGACCTACTGCCTCAATGT	AAGCACCATAGCCATCAACAC
Dct[d]	Cat	GAGCCTGCATAACTTGGTTCA	ATCCACAGGAGGATTGGATCT
Taqpep[d]	Cat	TGGCAGCGTTACAAGATGAC	ACTTCAGATTCCGCCACAAC
Mitf[d]	Cat	CTATAGCGTCCCCACGAAAA	TTTCTTCCATGCTCATGCTG
Slc7a11[d]	Cat	GCCCATTACCAGCTTTCGTA	CACGGCTGTAATGAGCTTGA

[a] For studies of mRNA expression by qPCR in *Tg.TRE-Edn3* mice (Fig. 4D)

[b] For studies of *Taqpep* mRNA expression by qPCR in mice (Fig. S6)

[c] For studies of *Edn3* mRNA expression by in situ hybridization in cats (Fig. 4C)

[d] For studies of mRNA expression by qPCR in cats, cheetahs, and leopards (Fig. 4C, S5C)

Supplemental Figure 1

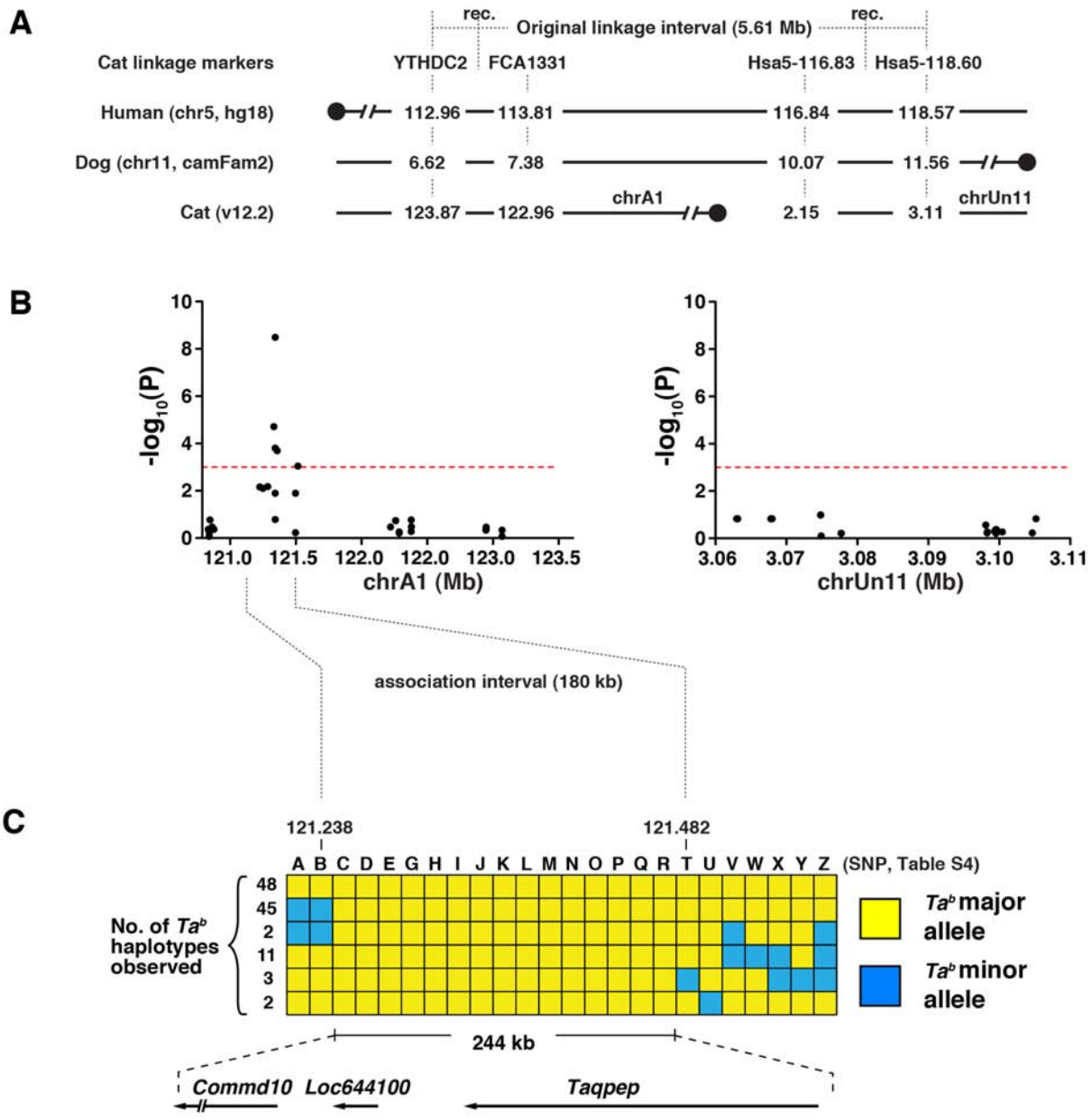

Fig S1. Genetic mapping of the *Tabby* gene. (A) Recombination (rec.) breakpoints for the *Tabby* linkage region lie on chromosome A1 and an unassigned contig (chrUn11), and correspond to a candidate interval of ~ 5 Mb in the dog (chr11: 6.62-11.56 Mb) and human (chr5: 112.96-118.60 Mb) genomes. (B) Significance of genotype-phenotype association, plotted as $-\log_{10}(P)$ from a chi-square test of allele counts is shown as a function of distance along chrA1 or chrUn11 for 58 SNPs (Table S4) in Ta^b/Ta^b (n = 8-16) compared to $Ta^M/-$ (n = 9-32) random-bred animals. The dashed red line indicates a Bonferroni-corrected 5% significance level. (C) Haplotype analysis (Table S4) narrows the interval to a 244 kb region (chrA1:121238572-121482501) containing 3 genes. The 111 Ta^b chromosomes summarized here do not include 5 singletons; all Ta^b chromosomes are shown separately in Fig. S2.

Supplemental Figure 2

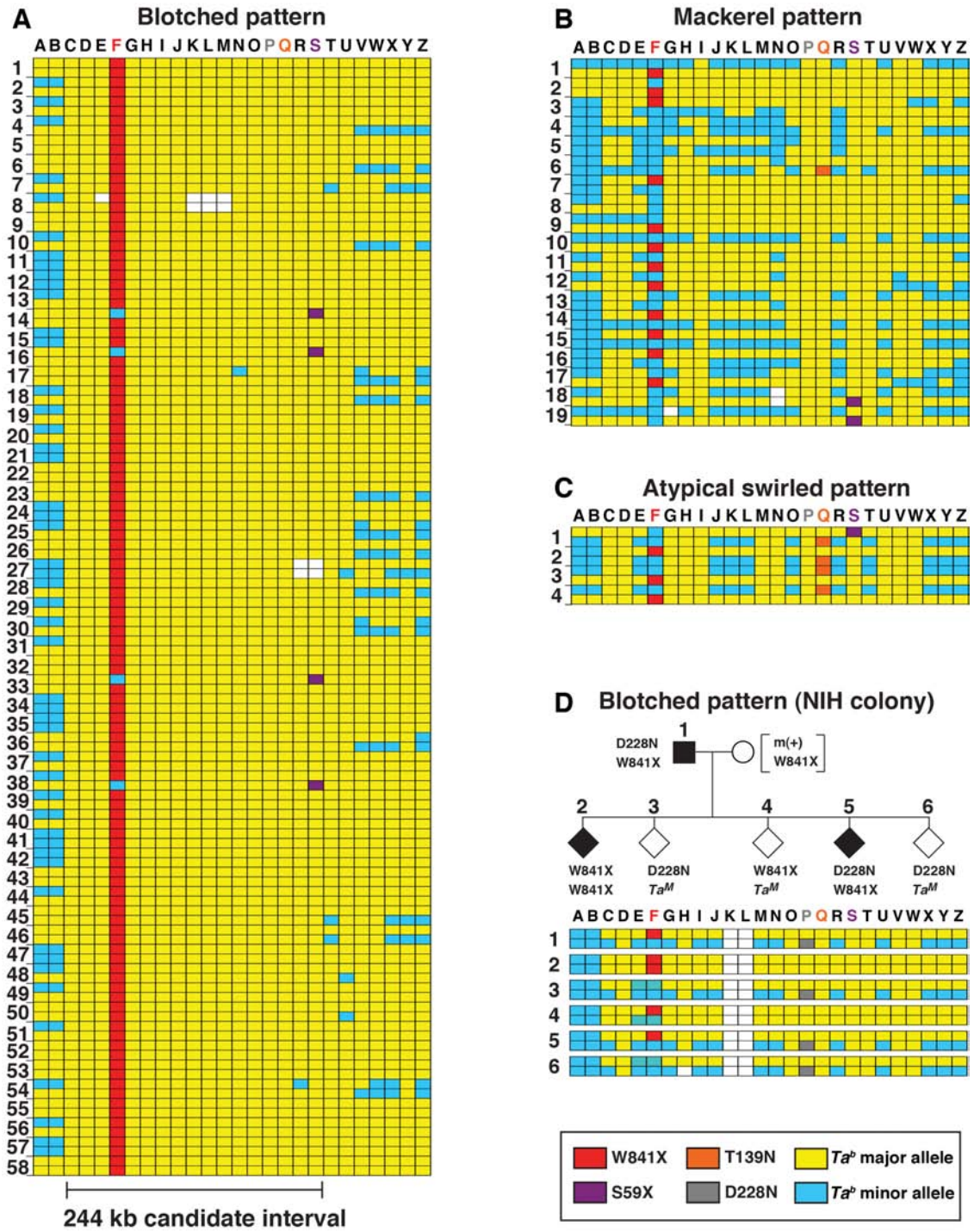

Fig. S2. Haplotypes for tabby patterns. Phenotypes are shown in Fig. 1 (blotched, mackerel) and Fig. S4D (atypical swirled). The S59X, T139N, and W841X alleles were observed in feral cats from a Northern California population (A, B, C) and also in breed cats (Table S2); the D228N mutation was observed only in animals from an NIH colony (D). SNP positions and genotyping information are given in Table S4.

Supplemental Figure 3

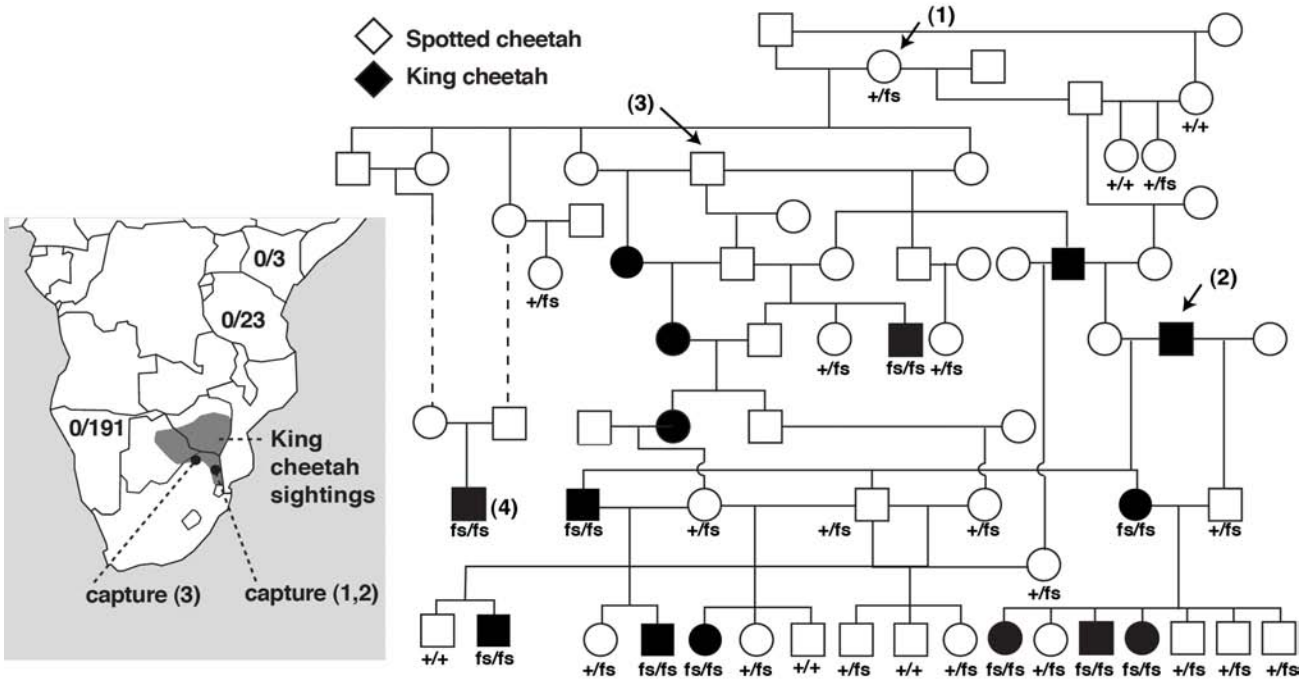

Fig. S3. (Left) King cheetah sightings have been restricted to a small (grey-colored) region that includes the Northeast corner of South Africa and parts of Botswana and Zimbawe. (Right) The K977Nfs110 mutation is completely linked to the king cheetah pattern (LOD = 5.7, $\theta = 0$) under a model of autosomal recessive inheritance with complete penetrance. Genotype results are shown for 32 captive animals from the DeWildt pedigree (non-mutant, +, or mutant, fs), and reveal that the frameshift mutation was introduced into the DeWildt pedigree by 3 captured animals (1-3). The proband animal from Northern California (4) is also derived from the DeWildt pedigree; dashed lines indicate 5 generations in which no king cheetahs were observed.

Supplemental Figure 4

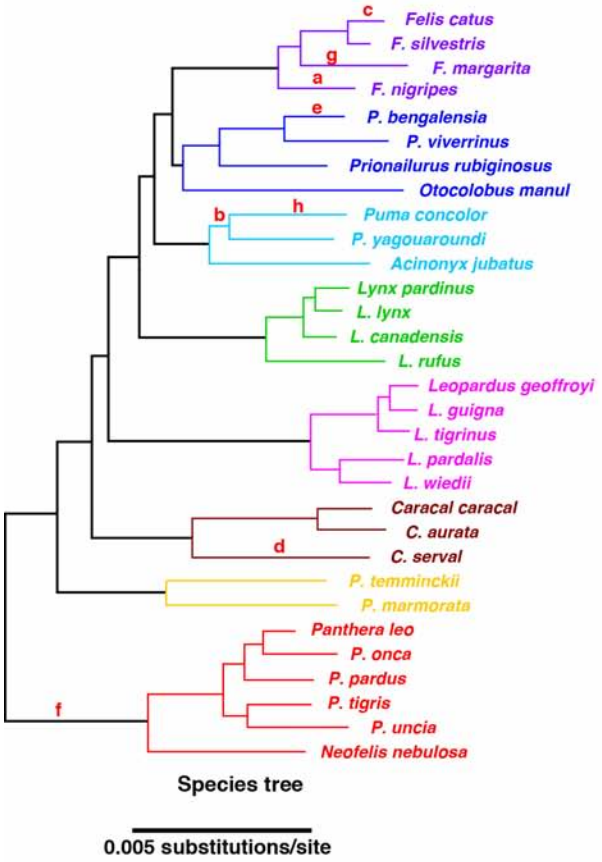

B

Position	82	110	139	228	282	603	817	880	950	975	989
Human	T	L	T	D	Q	R	E	A	F	L	R
Rhesus	T	L	T	D	Q	Q	E	A	F	L	R
Mouse	G	L	A	D	Q	Q	E	A	F	L	R
Guinea Pig	P	L	T	D	Q	Q	K	A	F	L	R
Horse	A	L	I	D	Q	Q	E	A	F	L	R
Dog	T	L	T	D	E	R	E	A	F	L	R
Microbat	T	L	T	D	Q	Q	E	A	F	L	R
Felid Mut.	K	V	N	N	E	S	G	V	V	V	W
Location	a	b	c	c	d	e	f	g	a	f	h
MAPP sc.	25	26	11	14	12	13	11	14	18	26	12
P value	***	***	*	**	*	**	*	**	**	***	*

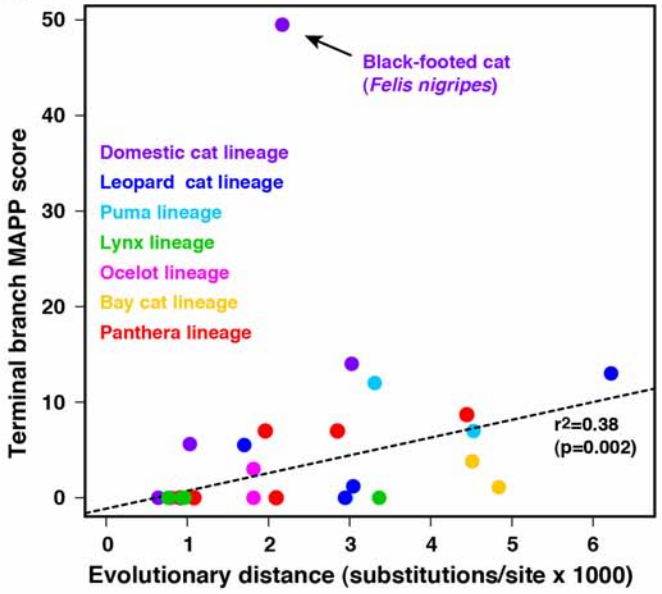

Fig S4. *Taqpep* variation during felid evolution. (A) Phylogeny of 31 felid species for which *Taqpep* sequence was determined, together with the inferred location of selected *Taqpep* substitutions depicted in panel (B). Topology and branch lengths for the tree are based on Johnson et al. (*36*) (B), Non-synonymous substitutions predicted to have a significant impact on protein function (MAPP score >10). Their assignment to branch locations on the felid tree is based on a maximum likelihood analysis in the context of a known phylogeny (A) as described in Methods. *, **, and *** indicate *P* values $< 5 \times 10^{-3}$, $< 5 \times 10^{-4}$, and $< 5 \times 10^{-5}$, respectively. (C) The potential impact of substitutions in each of 31 terminal branches (determined by the sum of MAPP scores for that branch) plotted as a function of terminal branch length based on (A). Species are organized into 7 main lineages according to Johnson et al. The regression line is based on all points except *F. nigripes* (the black-footed cat). (D) Pattern phenotype of *F. nigripes*, which resembles the atypical swirled pattern observed in domestic cats that carry the T139N allele (Fig. S2). Nine of nine *F. nigripes* individuals were fixed for 4 species-specific variants (T82K, H87P, E488K, F950V). Photographs were available for 4 of the 9 individuals that were sequenced (right-hand four panels); DNA was not available for the individual depicted in the upper left panel (from Pierre de Chabannes for www.photozoo.org).

Supplemental Figure 5

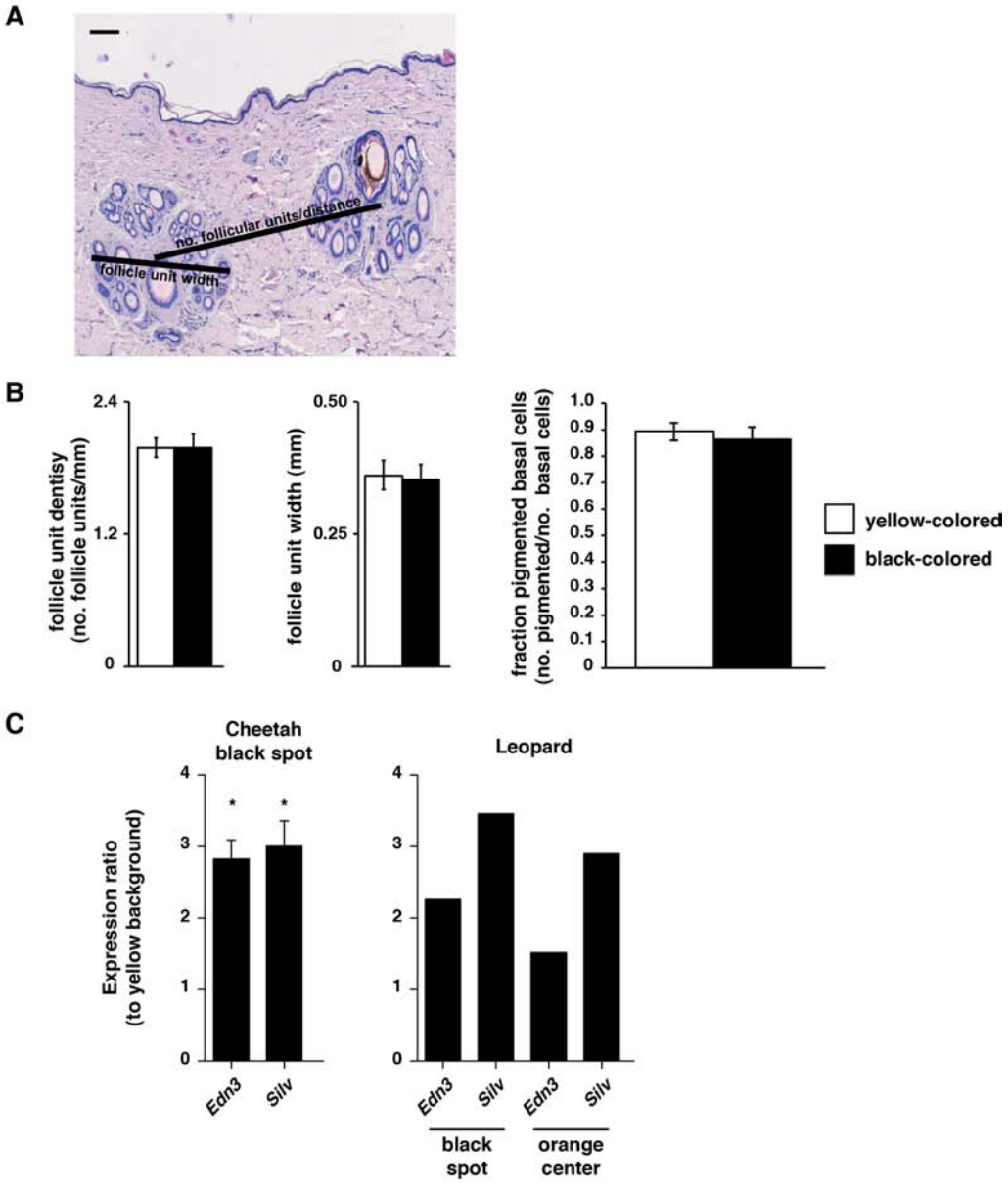

Fig. S5. Pattern characteristics of wild cat skin. (A) Hematoxylin and eosin-stained section of cheetah skin that includes a cross-section of complex follicle clusters from black (left) and yellow (right) colored areas. Scale bar: 100 uM. (B) Follicle density, follicle width, and the density of interfollicular epidermal cells (mean ± standard error) are indistinguishable between black- and yellow-colored areas. (C) Ratio of *Edn3* and *Silv* mRNA levels in cheetah (n=4) and leopard (n=1) skin regions, compared to the inter-spot yellow background areas. * $P<0.05$ (spot vs. background, two-tailed t test). The cheetah samples used here are distinct from those used for gene expression profiling (Fig. 5B).

Supplemental Figure 6

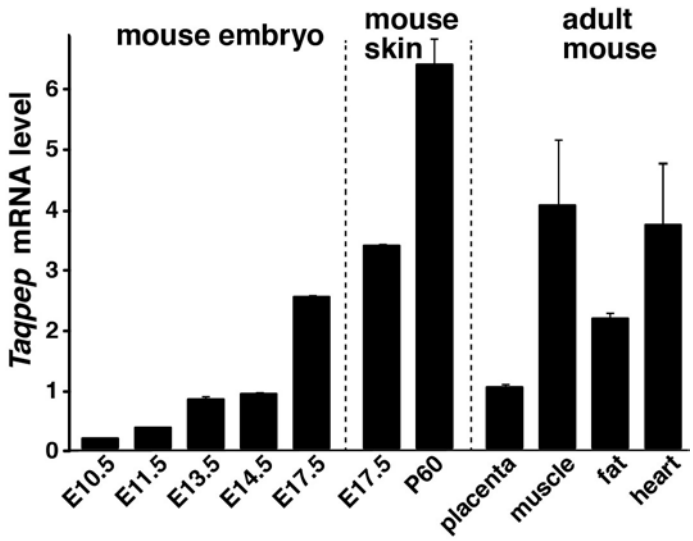

Fig. S6. Relative *Taqpep* mRNA levels in the laboratory mouse, measured by qRT-PCR from whole embryos, from embryonic (E17.5) and adult (P60) skin, and from other tissues. Results shown represent the mean ± standard error of three animals.

Supplemental Figure 7

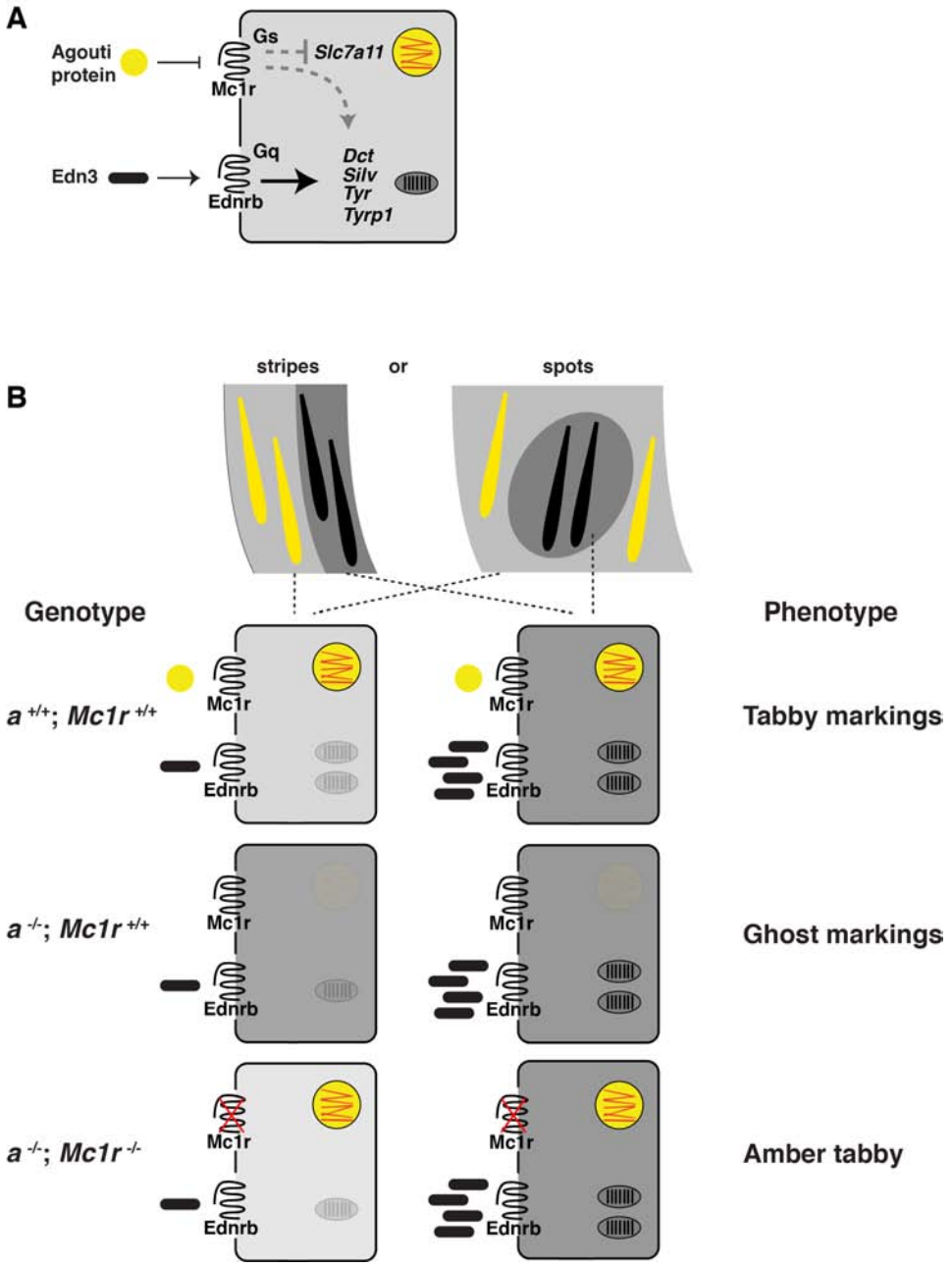

Fig. S7. Effects and interactions of endothelin and melanocortin signaling in cats. (A) The ability of *Edn3* to engage downstream eumelanic components is likely due to overlap between targets of Gs and Gq, the G proteins utilized by the Mc1r and Ednrb, respectively. The cartoon represents a single melanocyte. Red/yellow pheomelanosomes are produced when expression of *Slc7a11* is increased, and expression of *Dct*, *Silv*, *Tyr*, and *Tyrp1* are decreased; conversely, black/brown eumelanosomes are produced when expression of *Slc7a11* is decreased, and expression of *Dct*, *Silv*, *Tyr*, and *Tyrp1* are increased. (B) Interactions between *Agouti* and *Mc1r* in the context of tabby markings. Amber tabby cats exhibit strong tabby markings as kittens that fade during maturation (*5*). Diagrams are based on the expression results reported here (Fig. 4) and on ref. (*5*, *6*, *14*, *15*).

References

1. T. D. Lomax, R. Robinson, Tabby pattern alleles of the domestic cat. *J. Hered.* **79**, 21 (1988). Medline

2. A. G. Searle, *Comparative Genetics of Coat Color in Mammals* (Academic Press, New York, 1968).

3. S. E. Millar, M. W. Miller, M. E. Stevens, G. S. Barsh, Expression and transgenic studies of the mouse agouti gene provide insight into the mechanisms by which mammalian coat color patterns are generated. *Development* **121**, 3223 (1995). Medline

4. I. J. Jackson, Molecular and developmental genetics of mouse coat color. *Annu. Rev. Genet.* **28**, 189 (1994). doi:10.1146/annurev.ge.28.120194.001201 Medline

5. M. Peterschmitt, F. Grain, B. Arnaud, G. Deléage, V. Lambert, Mutation in the melanocortin 1 receptor is associated with amber colour in the Norwegian Forest Cat. *Anim. Genet.* **40**, 547 (2009). doi:10.1111/j.1365-2052.2009.01864.x Medline

6. E. Eizirik *et al*., Molecular genetics and evolution of melanism in the cat family. *Curr. Biol.* **13**, 448 (2003). doi:10.1016/S0960-9822(03)00128-3 Medline

7. E. Eizirik *et al*., Defining and mapping mammalian coat pattern genes: Multiple genomic regions implicated in domestic cat stripes and spots. *Genetics* **184**, 267 (2010). doi:10.1534/genetics.109.109629 Medline

8. C. A. Driscoll *et al*., The Near Eastern origin of cat domestication. *Science* **317**, 519 (2007). doi:10.1126/science.1139518 Medline

9. M. Maruyama *et al*., Laeverin/aminopeptidase Q, a novel bestatin-sensitive leucine aminopeptidase belonging to the M1 family of aminopeptidases. *J. Biol. Chem.* **282**, 20088 (2007). doi:10.1074/jbc.M702650200 Medline

10. R. I. Pocock, *Proc. Zool. Soc. London* **97**, 245 (1927).

11. R. J. van Aarde, A. van Dyk, *J. Zool.* **209**, 573 (1986).

12. E. A. Stone, A. Sidow, Physicochemical constraint violation by missense substitutions mediates impairment of protein function and disease severity. *Genome Res.* **15**, 978 (2005). doi:10.1101/gr.3804205 Medline

13. L. Z. Hong, J. Li, A. Schmidt-Küntzel, W. C. Warren, G. S. Barsh, Digital gene expression for non-model organisms. *Genome Res.* **21**, 1905 (2011). doi:10.1101/gr.122135.111 Medline

14. C. S. April, G. S. Barsh, Skin layer-specific transcriptional profiles in normal and recessive yellow (Mc1re/Mc1re) mice. *Pigment Cell Res.* **19**, 194 (2006). doi:10.1111/j.1600-0749.2006.00305.x Medline

15. T. Kobayashi *et al*., Modulation of melanogenic protein expression during the switch from eu- to pheomelanogenesis. *J. Cell Sci.* **108**, 2301 (1995). Medline

16. C. D. Van Raamsdonk, K. R. Fitch, H. Fuchs, M. H. de Angelis, G. S. Barsh, Effects of G-protein mutations on skin color. *Nat. Genet.* **36**, 961 (2004). doi:10.1038/ng1412 Medline

17. C. D. Van Raamsdonk, G. S. Barsh, K. Wakamatsu, S. Ito, *Pigment Cell Melanoma Res.* **22**, 819 (2009).

18. R. J. Garcia *et al*., Endothelin 3 induces skin pigmentation in a keratin-driven inducible mouse model. *J. Invest. Dermatol.* **128**, 131 (2008). doi:10.1038/sj.jid.5700948 Medline

19. A. Nakamasu, G. Takahashi, A. Kanbe, S. Kondo, Interactions between zebrafish pigment cells responsible for the generation of Turing patterns. *Proc. Natl. Acad. Sci. U.S.A.* **106**, 8429 (2009). doi:10.1073/pnas.0808622106 Medline

20. M. Iwashita *et al*., Pigment pattern in jaguar/obelix zebrafish is caused by a Kir7.1 mutation: Implications for the regulation of melanosome movement. *PLoS Genet.* **2**, e197 (2006). doi:10.1371/journal.pgen.0020197 Medline

21. M. Watanabe *et al*., Spot pattern of leopard Danio is caused by mutation in the zebrafish connexin41.8 gene. *EMBO Rep.* **7**, 893 (2006). doi:10.1038/sj.embor.7400757 Medline

22. H. Li, J. Ruan, R. Durbin, Mapping short DNA sequencing reads and calling variants using mapping quality scores. *Genome Res.* **18**, 1851 (2008). doi:10.1101/gr.078212.108 Medline

23. J. U. Pontius *et al*.; Agencourt Sequencing Team; NISC Comparative Sequencing Program, Initial sequence and comparative analysis of the cat genome. *Genome Res.* **17**, 1675 (2007). doi:10.1101/gr.6380007 Medline

24. J. C. Mullikin *et al*.; NISC Comparative Sequencing Program, Light whole genome sequence for SNP discovery across domestic cat breeds. *BMC Genomics* **11**, 406 (2010). doi:10.1186/1471-2164-11-406 Medline

25. The Genome Institute at Washington University, http://genome.wustl.edu/genomes/view/felis_catus/ (2011).

26. B. W. Davis *et al*., A high-resolution cat radiation hybrid and integrated FISH mapping resource for phylogenomic studies across Felidae. *Genomics* **93**, 299 (2009). doi:10.1016/j.ygeno.2008.09.010 Medline

27. M. Menotti-Raymond *et al*., An autosomal genetic linkage map of the domestic cat, *Felis silvestris catus*. *Genomics* **93**, 305 (2009). doi:10.1016/j.ygeno.2008.11.004 Medline

28. M. Stephens, N. J. Smith, P. Donnelly, A new statistical method for haplotype reconstruction from population data. *Am. J. Hum. Genet.* **68**, 978 (2001). doi:10.1086/319501 Medline

29. M. Fishelson, D. Geiger, Exact genetic linkage computations for general pedigrees. *Bioinformatics* **18** (suppl. 1), S189 (2002). doi:10.1093/bioinformatics/18.suppl_1.S189 Medline

30. M. D. Robinson, D. J. McCarthy, G. K. Smyth, edgeR: A Bioconductor package for differential expression analysis of digital gene expression data. *Bioinformatics* **26**, 139 (2010). doi:10.1093/bioinformatics/btp616 Medline

31. J. D. Storey, The positive false discovery rate: A Bayesian interpretation and the q -value. *Ann. Stat.* **31**, 2013 (2003). doi:10.1214/aos/1074290335

32. M. D. Abramoff, P. J. Magalhães, S. J. Ram, *Biophotonics International* **11**, 36 (2004).

33. J. L. Dards, R. Robinson, Gene frequencies in a population of feral cats in Portsmouth naval Dockyard. *Theor. Appl. Genet.* **64**, 197 (1983). doi:10.1007/BF00303764

34. A. G. Searle, Gene frequencies in London's cats. *J. Genet.* **49**, 214 (1949). doi:10.1007/BF02986074

35. N. B. Todd, Cats and commerce. *Sci. Am.* **237**, 100 (1977). doi:10.1038/scientificamerican1177-100

36. W. E. Johnson *et al.*, The late Miocene radiation of modern Felidae: A genetic assessment. *Science* **311**, 73 (2006). doi:10.1126/science.1122277 Medline